Available online at www.sciencedirect.com
SCIENCE DIRECT®
Journal of Organometallic Chemistry 690 (2005) 5125–5144
Journal of Organometallic Chemistry
www.elsevier.com/locate/jorganchem

Radical and migratory insertion reaction mechanisms in Schiff base zirconium alkyls

Paul D. Knight [a], Guy Clarkson [a], Max L. Hammond [a], Brian S. Kimberley [b], Peter Scott [a,*]

[a] Department of Chemistry, University of Warwick, Gibbett Hill Road, Coventry CV4 7AL, UK
[b] Research & Technology Centre, BP Chemicals snc, Boite Postale No. 6, 13117 Lavera, France

Received 9 February 2005; received in revised form 22 March 2005; accepted 23 March 2005
Available online 4 May 2005

Abstract

Four salicylaldimine derivatives $H_2\mathbf{L}^{4-7}$ of 2,2′-diamino-6,6′-dimethylbiphenyl, where the C=N bond is sterically protected by substituents on the phenol ring, form alkyls of zirconium, *cis*-α-[Zr$\mathbf{L}^{4-7}$($CH_2Ph)_2$]. Rather than decomposing via the established pathway of 1,2-migratory insertion of an alkyl group to imine, they undergo a radical mechanism. This is evidenced by the large number of products observed, kinetic and thermodynamic data (Rice-Herfeld, 3/2 order, positive $\Delta S^{\ddagger}$), response to steric factors, and the fact that switching to a less stable radical leaving group inhibits the reaction. In contrast, the 1,2-migratory insertion is a clean, first-order intramolecular process with negative $\Delta S^{\ddagger}$. The steric modification of the ligands nevertheless transforms an inactive precatalyst into a stable system for the polymerisation of ethene. Closely related unbridged salicylaldimine catalysts are known to be highly active catalysts, but in most cases they appear to suffer from high temperature instability. The first examples of zirconium alkyls of this class are isolated, and it is found that they are inherently much more resistant to decomposition by either pathway (migratory insertion or radical). Structural studies are used to interpret this variance in behaviour; the biaryl-bridged complexes are pre-organised for both reactions, while the unbridged systems would have to undergo significant ordering prior to activation. Correspondingly, the unbridged systems are not noticeably affected by the same steric modification of the ligand, and it is concluded that the more likely mechanism of catalyst death in the latter is ligand loss (i.e. transfer to aluminium from co-catalyst).

Keywords: Mechanism kinetics; Zirconium; Alkene polymerisation

1. Introduction

A fundamental concern for those using Schiff base complexes in catalytic applications is the reactivity of the C=N bond, specifically where this limits the number of turnovers. This issue is particularly important in early transition chemistry, where coordination of the imine unit renders it highly electrophilic [1]. We have sought to avoid this issue through the replacement of the C=N units with less reactive linkers, and while this has met with some successes in enantioselective catalysis [2], the favourable properties of Schiff base systems – strong ligand–metal bond, ease of synthesis, tunability, crystallinity, structural rigidity – have encouraged us to investigate the possibilities for improvement of their stability in early transition complexes. In this context, salicylaldimine (SA) complexes of the group 4 metals, [$M(SA)_2Cl_2$] (Fig. 1), which when combined with, e.g. methylaluminoxane (MAO) yield extremely active or otherwise useful catalysts for the polymerisation of alkenes, are of particular interest [3]. It is assumed that metal alkyls are involved in these catalyses, and evidence

* Corresponding author. Tel.: +44 24 7652 3238; fax: +44 24 7657 2710.
E-mail address: peter.scott@warwick.ac.uk (P. Scott).

0022-328X/$ - see front matter © 2005 Elsevier B.V. All rights reserved.
doi:10.1016/j.jorganchem.2005.03.043

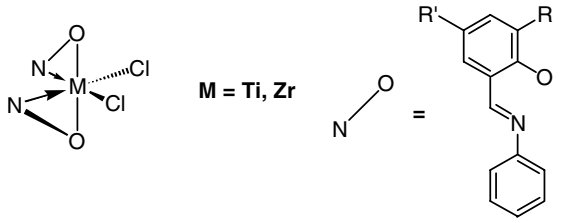

Fig. 1. Group 4 salicylaldimine complexes.

has been presented that alkyl cation species $[M(SA)_2Me]^+$ are formed on treatment of $[M(SA)_2Cl_2]$ with MAO [4]. Coates has mentioned that analogous ketimino ligands form stable alkyl complexes on treatment with $[Ti(CH_2Ph)_4]$ [5]. In contrast with many other olefin polymerisation systems however an alkyl cation has not been isloated.

We have recently shown that biaryl-bridged salicylaldimine derivatives $H_2\mathbf{L}^{1-3}$ (Fig. 2) form, under appropriate conditions, isolable alkyls of zirconium $[Zr\mathbf{L}^{1-3}R_2]$ with *cis*-α geometry (C_2-symmetric with *cis* alkyl ligands) [7]. Subsequently, however, they decompose via 1,2-migratory insertion of an alkyl group to imine (Scheme 1) followed in some instances by a second similar reaction. This provides an explanation for their complete inactivity in olefin polymerisation. Here we report a detailed kinetic investigation of this reaction, an attempt to prevent the process by ligand modification, discovery of a new decomposition mechanism, and the development of a stable polymerisation catalyst system. We also describe some attempts to apply the lessons learned to the SA catalyst system. Part of this work has been briefly communicated [6].

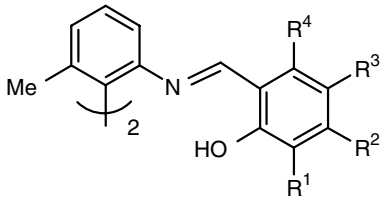

All R = H except:

$H_2\mathbf{L}^{1}$ $R^1 = R^3 = Me$

$H_2\mathbf{L}^{2}$ $R^1 = {}^iPr$

$H_2\mathbf{L}^{3}$ $R^3 = {}^tBu$

$H_2\mathbf{L}^{4}$ $R^1 = R^4 = Me$

$H_2\mathbf{L}^{5}$ $R^1 = Me$, $R^4 = {}^iPr$

$H_2\mathbf{L}^{6}$ $R^2 = R^4 = Me$

$H_2\mathbf{L}^{7}$ $R^1 = {}^iPr$, $R^4 = Me$

$H_2\mathbf{L}^{8}$ $R^1 = {}^tBu$, $R^4 = Me$

$H_2\mathbf{L}^{9}$ $R^1 = {}^tBu$, $R^3 = Me$

Fig. 2. Numbering scheme for proligands.

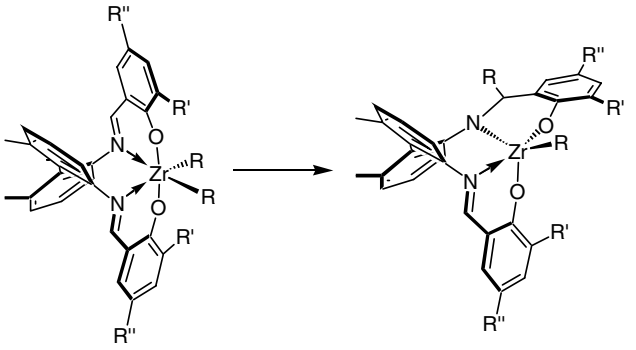

Scheme 1. 1,2-Migratory insertion of a metal bound benzyl group to an imine carbon [7].

2. Results and discussion

2.1. Ligand designs

Reducing the steric demand in the phenolate 2-position (R′ in Scheme 1) reduces the rate of 1,2-migratory insertion in the metal benzyl complexes $[Zr\mathbf{L}^n(CH_2Ph)_2]$ (i.e. $\mathbf{L}^3 < \mathbf{L}^1 < \mathbf{L}^2$) [7]. This is however an unsatisfactory resolution of the problem of complex stability for two reasons; (i) even when this group is hydrogen the 1,2-migratory insertion pathway is still accessible and occurs over a short period of time (<48 h), (ii) it is known that group 4 iminophenolate complexes require sterically demanding substituents (e.g. ^{t}Bu) in this position to furnish highly active catalysts for alkene polymerisation [3]. We thus sought other modifications.

A space-filling model of the molecular structure of $[Zr\mathbf{L}^1(CH_2Bu^t)_2]$ [7] is shown in Fig. 3(a), with the electrophilic imine carbon atom indicated ∗. We envisaged that notionally moving the 4-methyl substituent to the 5-position [Fig. 3(b)] would effectively block the approach of a zirconium bound alkyl group to the imine carbon atom. The series of ligands $\mathbf{L}^1$, $\mathbf{L}^4$, $\mathbf{L}^5$ was designed to examine the effect of steric demand in this 5-position. In addition, it was envisioned that the series $\mathbf{L}^6$, $\mathbf{L}^4$, $\mathbf{L}^7$ would allow investigation of the effect of steric demand in the 2-position for this unusual salicylaldimine substitution pattern.

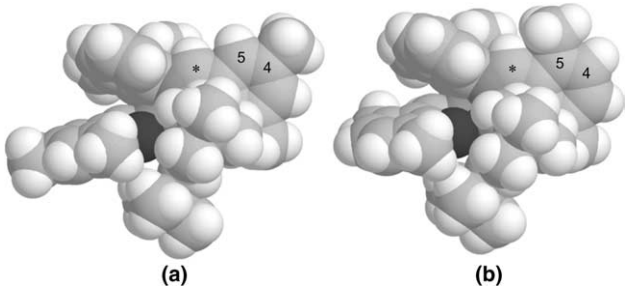

Fig. 3. Space-filling models of (a) $[Zr\mathbf{L}^1(CH_2CMe_3)_2]$ from X-ray molecular structure and (b) $[Zr\mathbf{L}^4(CH_2CMe_3)_2]$ based on (a); phenolate 4 and 5 positions and imine carbon atom (∗) indicated.

2.2. Synthesis of zirconium alkyl complexes

The synthesis of $[ZrL^1(CH_2Ph)_2]$ was reported previously [7]. Reaction of H_2L^4 with zirconium tetrabenzyl in acetonitrile yielded a precipitate which was found to be mainly unreacted H_2L^4. This was probably due to the low solubility of H_2L^4 in acetonitrile. The complex $[ZrL^4(CH_2Ph)_2]$ was successfully synthesised in dichloromethane at −78 °C. The reaction of the more soluble proligand H_2L^5 with $[Zr(CH_2Ph)_4]$ in acetonitrile proceeded cleanly giving $[ZrL^5(CH_2Ph)_2]$ in high purity. The complexes $[ZrL^6(CH_2Ph)_2]$ and $[ZrL^7(CH_2Ph)_2]$ were prepared similarly. The NMR spectra of freshly prepared solutions of these complexes were consistent with *cis*-α geometry.

2.3. Solution stability of $[ZrL^{4-7}(CH_2Ph)_2]$: initial observations

We were surprised to find that the four complexes $[ZrL^{4-7}(CH_2Ph)_2]$ underwent fairly rapid decomposition in solution, although the spectra of the products were markedly different from those expected for 1,2-migratory insertion processes. After ca. 3 h at 298 K, the ^1H NMR spectrum of a solution of $[ZrL^4(CH_2Ph)_2]$ in d_2-dichloromethane displayed a very large number of new peaks in the imine (δ 7.5–9.5 ppm) and aliphatic regions. These features, which were similar for all four complexes with a 5-substituent, are consistent with radical decomposition processes. Attempts at isolation of one of the many decomposition products were unsuccessful.

2.4. Kinetic studies of the decomposition processes

The decomposition of $[ZrL^1(CH_2Ph)_2]$ in d_2-dichloromethane was followed by ^1H NMR spectroscopy between 283 and 303 K. Values for the integration of the complex imine peak relative to the residual protio solvent resonance were obtained over ca. two half-lives where possible. First-order plots were satisfactory over the whole temperature range (Fig. 4). Similar variable temperature kinetic studies on the complexes $[ZrL^{4-7}(CH_2Ph)_2]$ showed that they did not decompose via first-order processes and after much experimentation it was found that the only satisfactory fit was via 1.5 order plots (e.g. Fig. 5). This unusual order was confirmed using Van't Hoff plots of the data.

Activation parameters (Table 1) were subsequently obtained via Eyring plots. The uncertainties recorded were calculated using standard methods [8].[1]

The negative value of entropy of activation for the decomposition of $[ZrL^1(CH_2Ph)_2]$ is consistent with the formation of an ordered (four-membered) cyclic transition state in an intramolecular 1,2-migratory insertion process. As we had proposed, placing a methyl group in the 5-position as in complex $[ZrL^4(CH_2Ph)_2]$ inhibits the formation of this cyclic transition state, but unexpectedly a new mechanistic pathway is opened up as evidenced by the number of products formed and by a change in the order of reaction to 3/2. Both observations are consistent with Rice–Herzfeld radical propagation kinetics [9,10] (vide infra).

We propose an initiation step involving homolytic fission of the Zr–CH_2Ph bond, leading to formation of two radical species (Eq. (1), Bn = CH_2Ph).[2] The benzyl radical can then attack the ligand (e.g. at an imine position) on another complex molecule to form a new radical species (Eq. (2)). We have previously described a very closely related reaction at a Nb(IV) Schiff base system (Scheme 2) leading to oxidation to diamagnetic Nb(V) [11]. In the case of Zr the radical character is retained by the ligands (Eq. (2)), and the system may react to form a closed shell complex and a further benzyl radical (Eq. (3)). The lack of a higher oxidation state for zirconium thus enables a radical propagation process that terminates when two radicals combine (Eq. (4)). Assuming steady state conditions, Eq. (5) is eventually obtained [10]. We note that the observed rate constant k_{obs} (Eq. (6)) and thus the thermodynamic values obtained from the Eyring analysis for the process of "activation" are actually *composite* parameters arising from initiation, propagation and termination. The positive entropies of activation for the complexes of L^{4-7} (Table 1) are nevertheless consistent with a radical process.

Initiation

$$[ZrL(Bn)_2] \xrightarrow{k_1} [ZrL(Bn)]^{\bullet} + Bn^{\bullet} \quad (1)$$

Propagation

$$Bn^{\bullet} + [ZrL(Bn)_2] \xrightarrow{k_2} [Zr(Bn\text{–}L)(Bn)_2]^{\bullet} \quad (2)$$

$$[Zr(Bn - L)(Bn)_2]^{\bullet} \xrightarrow{k_3} [Zr(Bn\text{–}L)(Bn)] + Bn^{\bullet} \quad (3)$$

Termination

$$Bn^{\bullet} + Bn^{\bullet} \xrightarrow{k_4} Bn_2 \quad (4)$$

$$\text{Rate} = k_2\left(\frac{k_1}{k_4}\right)^{0.5}[ZrL(Bn)_2]^{1.5} \quad (5)$$

$$\text{Rate} = k_{obs}[ZrL(Bn)_2]^{1.5} \quad (6)$$

[1] Standard error in the slope, $SE_m = s_e/\sqrt{TSS_x}$ and standard error in the intercept, $SE_c = s_e\sqrt{(1/n) + (\bar{X}^2/TSS_x)}$. These were computed using the LINEST function in Microsoft Excel.

[2] These equations are representative examples of the type of process described.

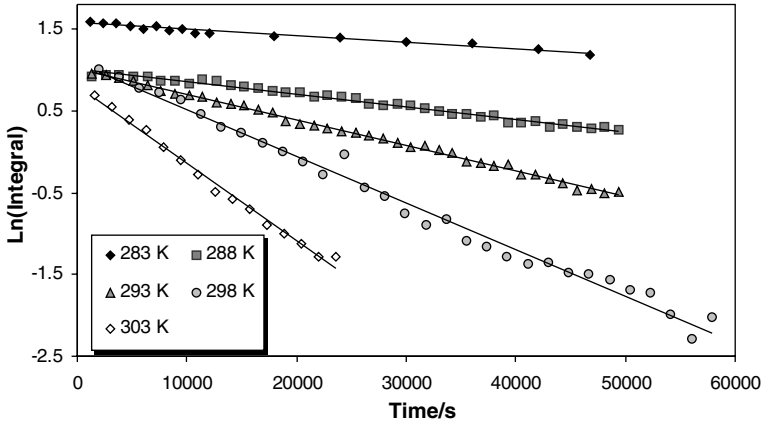

Fig. 4. First-order plots for decomposition of [Zr**L**^{1}(CH$_2$Ph)$_2$] at various temperatures.

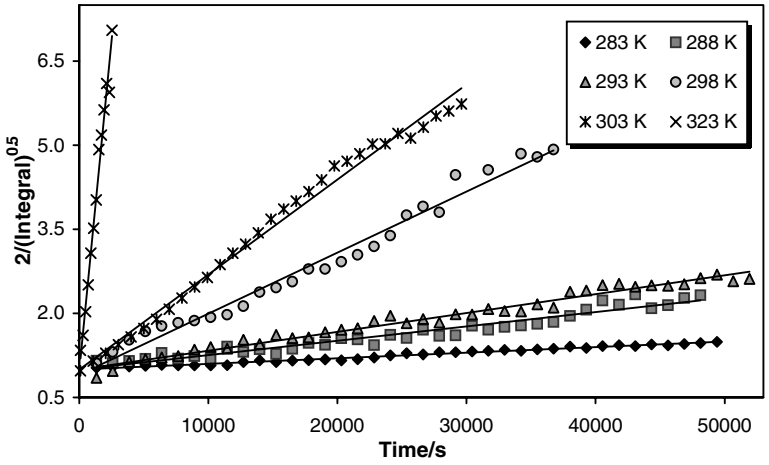

Fig. 5. Normalised 1.5 order plots for [Zr**L**^{4}(CH$_2$Ph)$_2$].

Table 1
Activation parameters and relative rates for decomposition of [Zr**L**^{n}(CH$_2$Ph)$_2$]

Complex	k_{rel} (298 K[a])	$\Delta H^{\ddagger}$ (kJ mol^{-1})	$\Delta S^{\ddagger}$ (J K^{-1} mol^{-1})
[Zr**L**^{1}(CH$_2$Ph)$_2$]	–	+88 (±2)	–32 (±7)
[Zr**L**^{4}(CH$_2$Ph)$_2$]	1.0	+101 (±5)	+16 (±16)
[Zr**L**^{5}(CH$_2$Ph)$_2$]	1.8	+113 (±10)	+62 (±34)
[Zr**L**^{6}(CH$_2$Ph)$_2$]	0.3	+108 (±7)	+29 (±23)
[Zr**L**^{7}(CH$_2$Ph)$_2$]	1.1	+91 (±5)	+17 (±16)

[a] Relative rate constant versus [Zr**L**^{4}(CH$_2$Ph)$_2$].

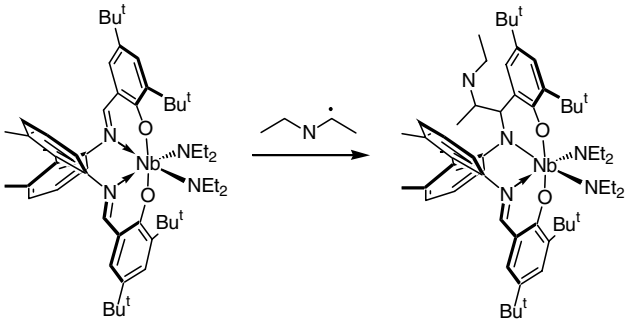

Scheme 2. Addition of diethylamine-2-yl radical to a Schiff base niobium (IV) complex.

Returning to the initiation step, we propose that the proximity of a benzylic H atom to the imine carbon may facilitate the homolytic fission of the metal–benzyl bond (Fig. 6). We note that the observed rate of decomposition of the **L**^{5} complex is almost twice that of **L**^{4} and this difference arises in the main from the much greater positive $\Delta S^{\ddagger}$ in the former where the proposed H atom donor unit is ^{i}Pr rather than Me.

Subject to the caveat mentioned above regarding the composite nature of the thermodynamic parameters, we also note that the enthalpies of activation decrease for the complexes in the order **L**^{6} > **L**^{4} > **L**^{7}, with steric bulk in the phenolate 2-position *increasing* in the same order (H < Me < ^{i}Pr). This is the same trend as observed for the first order 1,2-migratory insertion process and is consistent with greater steric compression in the more substituted complexes. The large increase in k_{rel} on

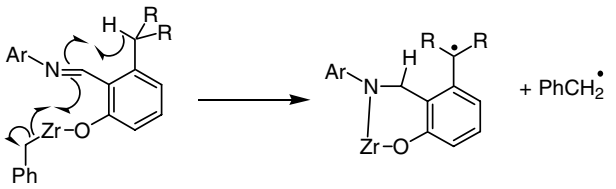

Fig. 6. Radical initiation mechanism.

moving from $\mathbf{L}^6$ to $\mathbf{L}^4$ is not continued on moving to $\mathbf{L}^7$ however, principally because the general trend in $\Delta S^{\ddagger}$ is acting against this.

2.5. Reaction of $H_2\mathbf{L}^4$ with $[Zr(CH_2CMe_3)_4]$

We explored briefly the effect of the presence of a less stable radical leaving group on the decomposition process. Reaction of $H_2\mathbf{L}^4$ with zirconium tetrakis(neopentyl) in dichloromethane proceeded smoothly, and a high purity sample of the complex $[Zr\mathbf{L}^4(CH_2CMe_3)_2]$ was obtained by crystallisation from pentane. This complex only began to show traces of decomposition in solution after leaving for several days at room temperature.

2.6. Synthesis and polymerisation activity of $[Zr\mathbf{L}^{1-7}Cl_2]$

Since the benzyl complexes were prone to decomposition, we attempted to generate the chloride complexes as these had previously been observed to be far more robust [12]. Treatment of the ligands with sodium hydride followed by $[ZrCl_4(THF)_2]$ proceeded without problem. The zirconium chloride complexes, $[Zr\mathbf{L}^{1-7}Cl_2]$, were then purified by sublimation at ca. 300 °C, 10^{-6} mm Hg in all cases and found to possess C_2 symmetry. However, treatment with MAO in toluene in the presence of ethylene at ambient temperature and 1.2 bar led to very low uptake of gas. This lack of activity may be attributed to the lack of steric bulk in the phenolate 2-position [3,13].

2.7. Synthesis of $[Zr\mathbf{L}^{8,9}Cl_2]$ and polymerisation catalysis

These zirconium chloride complexes were synthesised and characterised as before. Ethylene polymerisation results are summarised in Table 2. As can be seen, the presence of the phenolate 2-*tert*-butyl group in $[Zr\mathbf{L}^9Cl_2]$ does not give rise to significant polymerisation activity on its own. In combination with 5-methyl substituent, as in $[Zr\mathbf{L}^8Cl_2]$, polymerisation activity was observed for the first time using this type of ligand, albeit moderate according to Gibson's classification [14]. The catalyst is unusually stable, and there is no noticeable loss of activity at 25 and 50 °C over at least a period of 1 h (Fig. 7). The lower average productivity and activity at 50 °C is due to the reduced solubility of ethylene in toluene at higher temperatures.

2.8. Structural implications of phenolate 5-methyl substitution

We obtained X-ray molecular structures (Table 3) of $[Zr\mathbf{L}^7Cl_2]$ and $[Zr\mathbf{L}^9Cl_2]$ via crystals obtained from samples of the pure complexes in d_2-dichloromethane. The molecular structures are shown in Fig. 8 with selected bond lengths and angles given in Table 4. The view along the Zr–O axes (Fig. 9) highlights the influence of

Table 2
Polymerisation activity of complexes $[Zr\mathbf{L}^{8,9}Cl_2]$: precatalyst, 1.39×10^{-2} mmol; toluene (500 ml); ethene pressure, 1.2 bar; MAO:Zr molar ratio, 1000:1

Precatalyst	Temperature (°C)	Average productivity (1 h) (kg PE/mol–Zr bar–C_2 h)
$[Zr\mathbf{L}^8Cl_2]$	25	65
$[Zr\mathbf{L}^9Cl_2]$	25	–
$[Zr\mathbf{L}^8Cl_2]$	50	40
$[Zr\mathbf{L}^9Cl_2]$	50	–

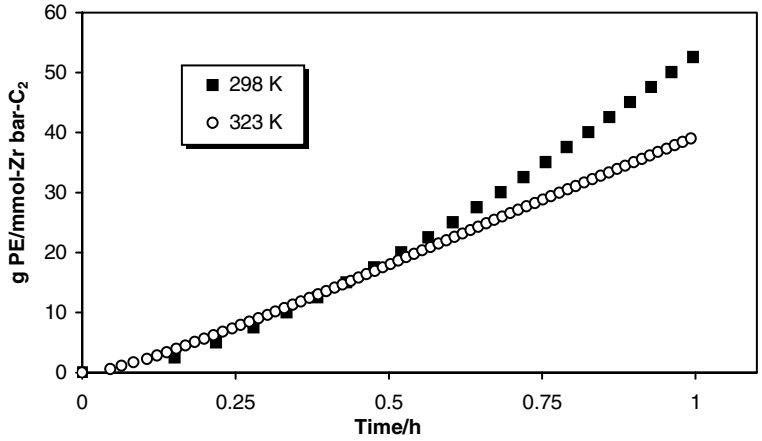

Fig. 7. Plot of ethene uptake vs. time/h for $[Zr\mathbf{L}^8Cl_2]$.

Table 3
Experimental data for the X-ray diffraction studies

	$[ZrL^7Cl_2]$	$[ZrL^9Cl_2]\cdot CH_2Cl_2$	$[ZrL^{11}Cl_2]$
Colour	Yellow	Yellow	Yellow
Habit	Block	Block	Block
Molecular formula	$C_{36}H_{38}Cl_2N_2O_2Zr$	$C_{39}H_{44}Cl_4N_2O_2Zr$	$C_{36}H_{40}Cl_2N_2O_2Zr$
Crystal system	Monoclinic	Monoclinic	Monoclinic
Space group	*C*2/*c*	*C*2/*c*	*C*2/*c*
a (Å)	19.975(4)	13.349(3)	21.166(4)
b (Å)	10.551(2)	14.379(3)	7.925(2)
c (Å)	15.521(3)	20.131(4)	20.282(4)
β (°)	97.95(3)	96.74(3)	100.770(19)
Cell volume (Å^3)	3239.7(11)	3837.4(13)	3342.2(14)
Z	4	4	4
μ (mm^{-1})	0.539	0.601	0.523
Total reflections	10,364	12,481	13,587
Independent reflections [*R*(int)]	3987 [0.0183]	4650 [0.1109]	4189 [0.0182]
R_1, wR_2 [$I > 2\sigma(I)$]	0.0235, 0.0617	0.0768, 0.1916	0.0225, 0.0585

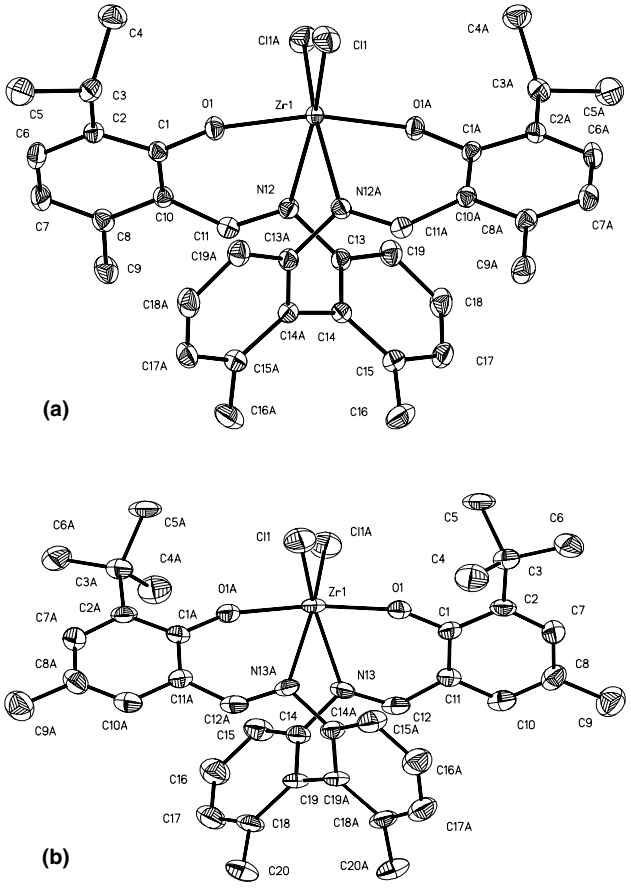

Fig. 8. Thermal ellipsoid plots of the molecular structures of (a) $[ZrL^7Cl_2]$ and (b) $[ZrL^9Cl_2]$.

the 5-methyl substituent; steric compression between this group and the imine-CH has led to a twist in the plane of coordination of the phenolate ring, such that the phenolate–CH_3 lies between the imine group and the adjacent Zr–Cl group. This increases the hindrance of the pathway for 1,2-migratory insertion between the imine carbon and a metal bound alkyl group (in place of Cl). This twisting of the phenolate ring may have an additional consequence in that the phenolate 2-alkyl substituent has been directed away from the "active sites" of the catalyst. This may reduce steric compression at these sites resulting in reduced propensity for decomposition as well as opening the sites for increased catalytic activity.

Table 4
Selected bond lengths (Å) and angles (°) for molecular structures of $[ZrL^7Cl_2]$, $[ZrL^9Cl_2]$ and *cis*-α-$[Zr(L^{11})_2Cl_2]$ (vide infra)

	$[ZrL^7Cl_2]$	$[ZrL^9Cl_2]$	$[Zr(L^{11})_2Cl_2]$
Zr–O	1.9987(11)	1.986(3)	1.981(9)
Zr–Cl	2.4246(6)	2.4313(17)	2.432(5)
Zr–N	2.3221(12)	2.347(4)	2.348(11)
O–Zr–O	165.30(6)	172.2(2)	157.40(5)
N–Zr–N	75.09(6)	72.9(2)	84.31(6)
Cl–Zr–Cl	103.82(3)	108.36(10)	94.38(3)

2.9. Synthesis and stability of active species in polymerisation catalysis

The question remained as to whether zirconium alkyl complexes of L^8 and L^9 decompose via different pathways. All attempts failed at generating the desired complexes by reaction of proligands with zirconium tetrabenzyl and zirconium tetrakis(neopentyl). ^{1}H NMR spectra indicated that the reaction was much slower than for less bulky ligands; resonances corresponding to unreacted and mono-deprotonated ligand were evident for the neopentyl reaction, and several other products were evident for the benzyl. Attempts at alkylation of the zirconium chloride complexes using Grignard and lithium reagents produced a number of unidentified products. Reactions of $[ZrL^8Cl_2]$ and $[ZrL^9Cl_2]$ in NMR tubes with previously dried MAO (10 molar equivalents) in d_8-toluene resulted in

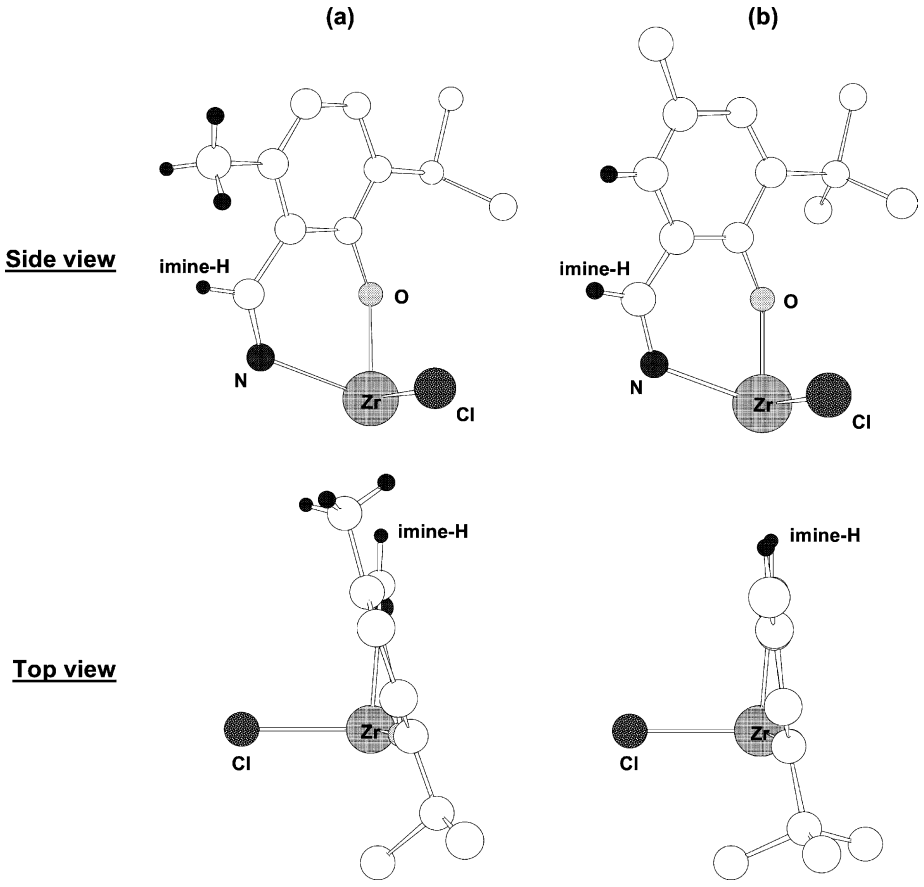

Fig. 9. Salicylaldimine–Zr–Cl fragments of (a) [Zr$\mathbf{L}^7Cl_2$] and (b) [Zr$\mathbf{L}^9Cl_2$] extracted from X-ray molecular structures, highlighting effects of substituents *ortho* to the imine carbon.

consumption of the starting complexes and significant broadening of the spectra, but no unambiguous indications of the formation of alkyl or alkyl cation species.

Since we could not generate zirconium alkyl complexes of $\mathbf{L}^8$ and $\mathbf{L}^9$, we decided to use complexes of $\mathbf{L}^4$ and $\mathbf{L}^1$ as models. An NMR tube was charged with [Zr$\mathbf{L}^1(CH_2Ph)_2$] and $B(C_6F_5)_3$, and d_2-dichloromethane was distilled into it at −78 °C. The ^{1}H NMR spectra were then recorded at −80 °C and then at increments of +10 °C up to room temperature. A similar reaction was carried out using [Zr$\mathbf{L}^4(CH_2Ph)_2$]. In both cases, the ^{1}H NMR spectra indicated formation of $[B(C_6F_5)_3(CH_2Ph)]^-$ [15]. Below ca. −40 °C, two imine peaks were observed that do not correspond to the starting complexes, and the presence of six methyl resonances indicate that the species formed were C_1 symmetric. For both reactions, new pairs of doublets occurred in the region δ 2.0–3.5 ppm, and we tentatively assign all these features to the desired cationic species $[Zr\mathbf{L}(CH_2Ph)]^+$. Upon warming the solution containing the proposed $\mathbf{L}^4$ complex cation, significant decomposition occurred between −30 and 0 °C; a large number of new imine peaks are generated and the pair of doublets disappeared. The solution containing the $\mathbf{L}^1$ complex also decomposes significantly within the same temperature range, however three major new imine peaks are observed along with the disappearance of the pair of doublets. No clear evidence for 1,2-migratory insertion processes was observed in either case.

2.10. Application to other catalyst systems

We sought to investigate the effect of 5-alkyl substitution on Fujita's zirconium iminophenolate catalysts. Four proligands H$\mathbf{L}^{10–13}$ (Fig. 10) were synthesised via

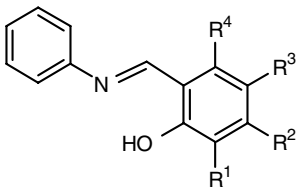

H$\mathbf{L}^{10}$ R^1 = ^{t}Bu, R^4 = Me
H$\mathbf{L}^{11}$ R^1 = ^{t}Bu, R^3 = Me
H$\mathbf{L}^{12}$ R^1 = R^4 = Me
H$\mathbf{L}^{13}$ R^1 = R^3 = Me

Fig. 10. Modified salicylaldimines and suitable control ligands.

condensation of the appropriate salicylaldehydes with aniline in ethanol. Two of these ligands ($HL^{10,12}$)have a methyl group in the 5-position and two control ligands $HL^{11,13}$ have the traditional 2,4-substitution (HL^{11} has previously appeared) [16].

Reactions of HL^{10} and HL^{11} with sodium hydride in THF followed by $[ZrCl_4(THF)_2]$ resulted in the production of yellow/orange solids which were sublimated at ca. 300 °C, 10^{-6} mm Hg to yield yellow solids of stoichiometry $[Zr(L^{10,11})_2Cl_2]$, as indicated by mass spectrometry and CHN analysis. ^{1}H NMR spectra revealed that two isomeric complexes were present in both cases. The major products were C_2-symmetric, as indicated by the presence of single imine, phenolate methyl and *tert*-butyl resonances. The minor products (ca. 27% for $[ZrL^{10}_2Cl_2]$ and ca. 36% for $[ZrL^{11}_2Cl_2]$) had broad ^{1}H NMR spectra at room temperature, but cooling (253 K for $[ZrL^{10}_2Cl_2]$ and 203 K for $[ZrL^{11}Cl_2]$) gave rise to sharp resonances. Two imine peaks and two phenolate methyl and *tert*-butyl resonances were observed in both complexes. We therefore assigned these species as having the C_1-symmetric *cis*-β topography. The ratio of *cis*-α to *cis*-β remains unchanged over a period of days. Interestingly, Fujita and coworkers [16] did not note the presence of *cis*-β isomers of $[ZrL^{11}Cl_2]$, although their NMR data are possibly consistent with this. Coates [5] has noted the presence of *cis*-β isomers of ketimino titanium complexes and others.

Crystals of *cis*-α-$[ZrL^{11}_2Cl_2]$ were grown from toluene solution. X-ray analysis revealed that the C_2-symmetric complex (Fig. 11) crystallises as a dimer via a face-face π–π stacking interaction between *N*-aryl rings (Fig. 12). The distance between H(16A) and the centroid of the proximal aryl ring is ca. 3.37 Å [17]. The bond distances and angles about Zr(1) are unremarkable for this type of complex [16] and are discussed in more detail through comparison with those of a biaryl-bridged complex in Section 2.12.

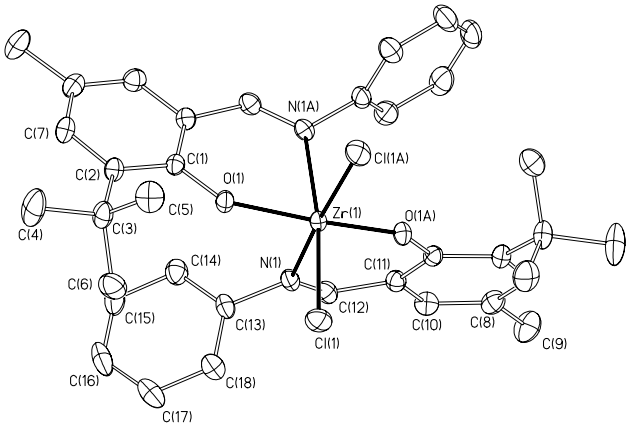

Fig. 11. X-ray molecular structure of *cis*-α-$[Zr(L^{11})_2Cl_2]$.

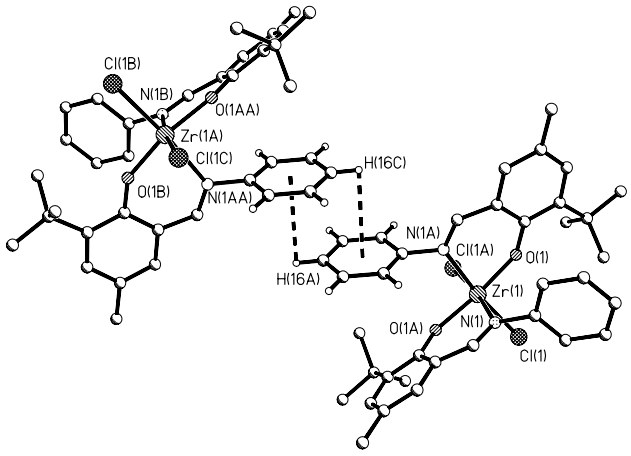

Fig. 12. Crystal packing between adjacent molecules of $[ZrL^{11}_2Cl_2]$.

Samples of $[ZrL^{10}_2Cl_2]$ and $[ZrL^{11}_2Cl_2]$ were tested at BP laboratories under supported gas-phase conditions with MAO co-catalyst. Both complexes had similarly high activities and catalytic lifetimes were <10 min at 50–80 °C in both instances. Thus, while substitution of the ligand with a methyl group *ortho* to the imine carbon atom does not significantly alter the intrinsic polymerisation activity of the complexes, it fails to increase longevity of the catalyst in this instance. In the hope of shedding further light on the issue of iminophenolate catalyst stability we undertook a study of some alkyl derivatives.

2.11. Synthesis and properties of $[Zr(L^{10–13})_2(CH_2Ph)_2]$

In NMR tube scale experiments, the reactions between two equivalents each of $HL^{10–13}$ with $[Zr(CH_2Ph)_4]$ were shown to give cleanly $[Zr(L^{10–13})_2(CH_2Ph)_2]$. One example, $[ZrL^{10}{}_2(CH_2Ph)_2]$, was synthesised on a preparative scale and was characterised in the usual way. Attempts to grow single crystals for X-ray analysis were unsuccessful.

The ^{1}H NMR spectrum of $[ZrL^{10}_2(CH_2Ph)_2]$ indicated the adoption of the *cis*-α structure; in particular the appearance of the CH_2Ph as a pair of AB doublets indicated that interconversion between the chiral-at-metal structures (Fig. 13) is slow on this

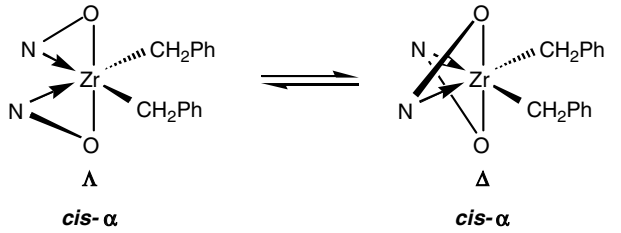

Fig. 13. Interconversion of complex enantiomers for *cis*-α-$[Zr(L^{10–13})_2(CH_2Ph)_2]$.

timescale. The spectrum of $[ZrL^{11}_2(CH_2Ph)_2]$ was similar. For $[Zr(L^{12,13})_2(CH_2Ph)_2]$ these CH_2Ph resonances appeared as a broad singlet. This trend in configurational stability is consistent with an *N*-dissociative mechanism since bulky groups in the phenolate 2-position would cause steric compression on lengthening of the N–Zr bond, and hence hinder isomerisation [18].

All the above complexes were found to be relatively stable with respect to the decomposition reactions detailed above. After several days in solution at ambient temperature, samples of the bulky ligand complexes $[Zr(L^{10,11})_2(CH_2Ph)_2]$ began to show signs of formation of 1,2-migratory insertion products, viz. a new single imine peak and a set of three quartets in the region ca.

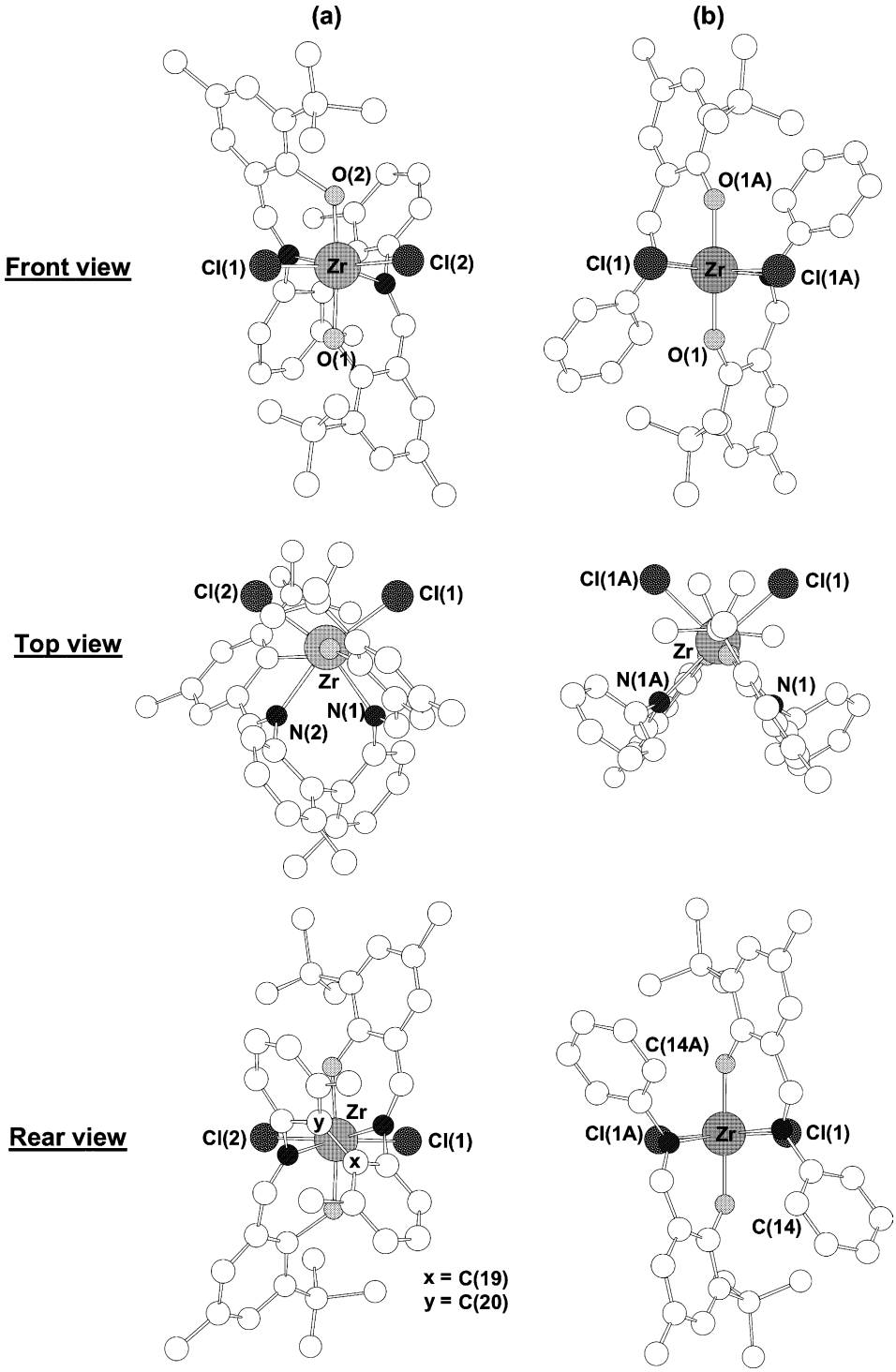

Fig. 14. Comparison of the molecular structures of *cis*-α-$[ZrL^{9}Cl_2]$ and *cis*-α-$[ZrL^{11}_2Cl_2]$.

δ 2.5–6.5 ppm [1a]. Solutions of the complexes $[Zr(\mathbf{L}^{12-13})_2(CH_2Ph)_2]$ showed very little, if any, decomposition over a period of several days.

2.12. Stability of $[Zr\mathbf{L}_2^{10}CH_2Ph]^+$

We attempted to generate an alkyl cation complex by reaction of $[Zr\mathbf{L}_2^{10}(CH_2Ph)_2]$ with $B(C_6F_5)_3$ in an NMR tube at −78 °C, using d_2-dichloromethane as solvent. ^1H NMR spectra were recorded at −80 °C and at +10 °C increments up to room temperature. Resonances for $[B(CH_2Ph)(C_6F_5)_3]^-$ were observed at low temperature [15], indicating that a reaction had taken place, but while some resonances assignable to a cationic species $[Zr(\mathbf{L}^{10})_2(CH_2Ph)]^+$ were observed, by −40 °C extensive decomposition had occurred. This result and the attempts to form $[Zr\mathbf{L}^{1,4}(CH_2Ph)]^+$ (Section 2.8), do not bode well for isolation of a stable alkyl cationic species such as that implicated in olefin polymerisation catalyses by these complexes. Fujita [4] has also detected NMR resonances consistent with such a species on treatment of a dichloride complex with dried MAO.

2.13. Biaryl-bridged complexes vs. non-bridged complexes

Complexes of our biaryl-bridged ligands above and the non-bridged salicylaldimine type ligands are similar in terms of functionality. Nevertheless, considerable differences are observed for polymerisation activity. We can see that in comparison to the constrained structure of the biaryl complex $[Zr\mathbf{L}^9Cl_2]$ [Fig. 14(a)], the *N*-aryl units in the non-bridged ligand complex $[Zr\mathbf{L}_2^{11}Cl_2]$ (b) are directed away from one another. The presence of the biaryl unit also constrains the N–Zr–N′ angle to ca. 72.9° compared with 84.3° for $[Zr\mathbf{L}_2^{11}Cl_2]$, (Table 4), and perhaps most importantly reduces the size of the active site by forcing the phenolate units forwards; the O–Zr–O′ angles for $[Zr\mathbf{L}^9Cl_2]$ and $[Zr\mathbf{L}_2^{11}Cl_2]$ are 172.2° and 157.4°, respectively. The top view of the complexes shows that the phenolate *tert*-butyl substituents are positioned directly above the zirconium chloride sites in the $\mathbf{L}^9$ complex, whereas in the $\mathbf{L}^{11}$ complex these *tert*-butyl groups are situated above the zirconium centre. The resultant steric compression in $[Zr\mathbf{L}^9Cl_2]$ forces the chlorides farther apart (108.4°) than in the $\mathbf{L}^{11}$ complex (94.4°). Given these structural differences, the variance in intrinsic catalytic activity between $[Zr\mathbf{L}^8Cl_2]$ and $[Zr\mathbf{L}_2^{10}Cl_2]$ is not surprising.

The variance in response of the two catalysts systems to attempted steric blocking of the 1,2-migratory insertion reaction also requires comment. For the biaryls, the geometry is essentially *pre-organised* for the approach of metal-coordinated alkyl towards the carbon atom. Steric compression from phenolic *ortho* substituents (top view, Fig. 14) encourages this further. Nevertheless, the constrained biaryl ligand geometry also dictates that a methyl group *ortho* to the imine consistently impedes this reaction, thus leading to the remarkable increase in catalyst stability detailed above. The unbridged complexes are not *pre-organised* for this reaction, and as a result the 1,2-migratory insertion is inherently slower for these compounds. The observation that phenolate 5-methyl substitution does not affect catalyst longevity suggests that either; (i) despite the fact that complexes $[Zr(\mathbf{L}^{10-13})_2(CH_2Ph)_2]$ appear to be rather stable with respect to 1,2-migratory insertion, the greater flexibility allows for imine migratory insertion even in the modified catalyst, or perhaps more likely (ii) that other processes are responsible for catalyst deactivation (vide infra).

3. Conclusions

Our attempt here to block sterically the 1,2-migratory insertion process in our Schiff base group 4 alkyl complexes was successful principally because of the lack of flexibility of the system. This also results however in the complexes being pre-organised for decomposition via a radical process. Kinetic analysis and ^1H NMR spectroscopy data highlight the differences between the two pathways. For the 1,2-migratory insertion mechanism a single product was formed in a highly diastereoselective intramolecular manner to give an unstable intermediate. The reaction displayed first order reaction kinetics with a negative entropy of activation associated with ordered transition state. The radical process gave many products in a 1.5 order Rice–Herzfeld reaction with positive entropy of activation, but was inhibited through the use of a less stable radical leaving group (neopentyl) at the metal, thus finally giving a stable metal alkyl.

The effect on polymerisation catalysis using the biaryl-bridged complexes with this ligand modification is significant as we transformed an inactive system to one that displays activity (albeit moderate) and also demonstrated that the catalyst is long lived.

Application of this simple ligand modification to the unbridged salicylaldimine systems did not lead to an increase in polymerisation catalyst lifetime at higher temperatures. At least two explanations are available which are consistent with observations to date. If imine reactivity is at the heart of the instability of the unbridged systems, then the lack of success in inhibiting 1,2-migratory insertion by our method might be traced to the differences in precatalyst structure detailed in Section 2.13. If on the other hand, loss of a salicylaldimine ligand (e.g. via transfer to aluminium from MAO) causes catalyst death, then this steric modification would not be expected to make a significant difference. We note the growing body of evidence for the latter picture, such as the relatively poor polymerising capabilities of mono-salicylaldimine complexes [19] and improved stability of more electron-rich phenolate systems [20].

It remains however that tetradentate systems have been shown here to yield a stable catalyst, and if this along with high activity and ability to polymerise α-olefins in a stereoselective manner is the goal, then attempts to balance ligand constraint and flexibility might be fruitful.

4. Experimental

4.1. General details

Unless stated otherwise, organic preparations were carried out in air. Organometallic manipulations were performed under an atmosphere of dry argon, using conventional Schlenk line techniques and an MBraun glove box (<1 ppm O_2/H_2O). For organometallic preparations, hydrocarbon and ether solvents were pre-dried over sodium wire. These were then dried under reflux conditions over sodium (for toluene), potassium (THF and benzene), sodium–potassium alloy (diethyl ether, petroleum ether and pentane), then distilled and degassed before use. Dichloromethane and acetonitrile were dried under reflux conditions over calcium hydride then distilled and degassed. Deuterated solvents were degassed by the freeze–thaw method and dried over potassium (toluene, benzene and THF) or calcium hydride (dichloromethane and acetonitrile) before trap-to-trap distillation and storage in the glove box. NMR samples of air sensitive species were prepared in the glovebox in tubes sealed with Young's concentric stopcocks.

Unless stated otherwise, commercial chemical reagents were used as received. Chiral ligands and complexes were racemic mixtures.

NMR spectra were recorded at ca. 298 K on Bruker AC-250, DPX-300, DPX-400 or AC-400 spectrometers and the spectra referenced internally using residual protio solvent resonances relative to tetramethylsilane ($\delta = 0.0$ ppm). Proton and carbon NMR assignments were confirmed routinely by ^1H–^1H (COSY) or ^1H–^{13}C (HMQC) experiments. NMR kinetic data were obtained using Bruker AC-400 or DPX-500 spectrometer with calibrated temperature probes. Infrared spectra were carried out on sodium chloride plates in an airtight holder, and obtained as thin film (dichloromethane as solvent) or nujol mulls on a Perkin–Elmer FT-IR spectrometer. EI and CI mass spectra were obtained on a VG Autospec mass spectrometer. Elemental analyses were performed by Warwick Analytical Services. For some alkyl complexes, analyses of %C were found to be lower than calculated values despite the use of high combustion temperatures and the addition of combustions aids; this is frequently the case in such systems [21].

The compounds $LiCH_2CMe_3$ [22], $[Zr(CH_2CMe_3)_4]$ [23] and $[Zr(CH_2Ph)_4]$ [24] were synthesised by literature methods.

4.2. Synthesis of salicylaldehydes [25]

The reaction was performed with rigorous exclusion of moisture. Acetonitrile and triethylamine were dried over CaH_2, paraformaldehyde was dried over P_2O_5 and "anhydrous" $MgCl_2$ was dried over P_2O_5 at 120 °C. A 1 l side arm round bottom flask with stirrer bar was placed under an argon atmosphere and charged with the appropriate phenol (100 mmol) and dry acetonitrile (500 ml). To this was added dry triethylamine (52.2 ml, 375 mmol), anhydrous $MgCl_2$ (14.28 g, 150 mmol) and the solution was stirred for 15 min. Dry paraformaldehyde (20.25 g, 675 mmol) was added and a wide bore condenser fitted to the round bottom flask. The solution was heated at reflux temperature under argon for ca. 2.5 h. The solution was allowed to cool to room temperature and added to 5% aqueous HCl (800 ml) followed by stirring for 30 min. This was extracted with diethyl ether (7 × 100 ml portions) and the ether fractions collected together and washed with saturated $NaCl_{(aq)}$ (3 × 100 ml portions). The ether layer was dried over anhydrous $MgSO_4$ followed by filtration. Volatiles were removed under reduced pressure to yield the corresponding salicylaldehydes, usually contaminated with the starting phenol. Purification prior to reaction with the biaryl diamine (vide infra) was found to be generally unnecessary since the Schiff base product precipitates from the reaction solution. Samples of the products were nevertheless isolated and fully characterised, as described below.

4.2.1. 2-Hydroxy-3,6-dimethylbenzaldehyde

Using the general procedure with 2,5-dimethylphenol (12.21 g), the reaction mixture was heated at reflux temperature for 3 h during which time the solution turned green. A yellow solid (14.92 g) was obtained, which was found to contain the target compound (90% by ^1H NMR) along with the starting phenol. A sample of the mixture (2.00 g) was purified by column chromatography using hexane:diethyl ether 4:1 as the eluent. Similar fractions (TLC analysis) were collected together and volatiles were removed under reduced pressure to leave a pale green crystalline solid (1.71 g).

Yield from 2.00 g or crude product = 1.71 g, 84%.

Anal. found (Calculated for $C_9H_{10}O_2$)% C 71.57 (71.99), H 6.73 (6.71).

^1H NMR 300 MHz ($CDCl_3$) δ ppm 12.17 (s, 1H, ArO*H*), 10.29 (s, 1H, *H*C=O), 7.23 (d, 1H, Ar*H*, $^3J_{HH} = 7$ Hz), 6.61 (d, 1H, Ar*H*, $^3J_{HH} = 7$ Hz), 2.56 (s, 3H, *Me*), 2.20 (s, 3H, *Me*).

$^{13}C\{^1H\}$ NMR 75 MHz ($CDCl_3$) δ ppm 195.4, 161.5, 139.3, 138.0, 124.9, 121.1, 117.8, 17.8, 14.8.

IR (CH_2Cl_2 thin film) ν cm^{-1} 2955, 1645 (s, C=O), 1626, 1513, 1462, 1432, 1408, 1376, 1330, 1280 (m, C–O), 1252, 1236, 1058, 1030, 974, 822, 775, 740, 696.

MS (EI) *m/z* 150 $[M]^+$, 149 $[M - H]^+$, 135 $[M - CH_3]^+$.

4.2.2. 2-Hydroxy-6-isopropyl-3-methylbenzaldehyde

Using the general procedure with 5-isopropyl-2-methylphenol (carvacrol) (15.4 ml), the mixture was heated at reflux temperature for 3.5 h during which time the solution turned yellow. A yellow/brown oil (17.24 g) was obtained and found to contain the target compound (75% by ^{1}H NMR). A sample of the oil (1.00 g) was purified by column chromatography (hexane:diethyl ether 4:1). Similar fractions (TLC analysis) were collected together and the solvent was removed under reduced pressure to leave a pale yellow/green oil (0.72 g).

Yield from 1.00 g of crude product = 0.72 g, 70%.

Anal. found (Calculated for $C_{11}H_{14}O_2$)% C 74.10 (74.13), H 7.99 (7.92).

^{1}H NMR 300 MHz ($CDCl_3$) δ ppm 12.42 (s, 1H, ArO*H*), 10.40 (s, 1H, *H*C=O), 7.31 (d, 1H, Ar*H*, $^3J_{HH}$ = 8 Hz), 6.76 (d, 1H, Ar*H*, $^3J_{HH}$ = 8 Hz), 3.60 (m, 1H, C*H*Me$_2$, $^3J_{HH}$ = 7 Hz), 2.20 (s, 3H, *Me*), 1.31 (d, 6H, CH*Me*$_2$, $^3J_{HH}$ = 7 Hz).

^{13}C{^{1}H} NMR 75 MHz ($CDCl_3$) δ ppm 195.1 (H*C*=O), 161.7, 150.2, 138.2, 124.3, 116.3, 115.5 (Ar), 27.2 (*C*HMe$_2$), 24.2 (CH*Me*$_2$), 14.9 (*Me*).

IR (CH_2Cl_2 thin film) ν cm^{-1} 2965, 2926, 2874, 1892, 1632 (s, C=O), 1584, 1457, 1425, 1407, 1314, 1266 (m, C–O), 1256, 1228, 1176, 1155, 1107, 1063, 1034, 976, 752, 870, 823, 787, 716, 693, 654, 545.

MS (EI) *m*/*z* 178 $[M]^+$, 177 $[M - H]^+$, 163 $[M - CH_3]^+$.

4.2.3. 2-Hydroxy-4,6-dimethylbenzaldehyde

Using the general procedure with 3,5-dimethylphenol (12.21 g), the mixture was heated at reflux temperature for 3 h, during which time the solution turned green. A yellow solid was obtained.

Yield = 14.75 g, 97%.

Anal. found (Calculated for $C_9H_{10}O_2$)% C 71.98 (71.98), H 6.62 (6.71).

^{1}H NMR 300 MHz ($CDCl_3$) δ ppm 11.93 (s, 1H, ArO*H*), 10.19 (s, 1H, *H*C=O), 6.59 (s, 1H, Ar*H*), 6.50 (s, 1H, Ar*H*), 2.52 (s, 3H, *Me*), 2.28 (s, 3H, *Me*).

^{13}C{^{1}H} NMR 75 MHz ($CDCl_3$) δ ppm 194.4 (H*C*=O), 163.2, 149.1, 141.7, 123.0, 116.4, 115.9 (Ar), 22.0, 17.8.

IR (CH_2Cl_2 thin film) ν cm^{-1} 3426 (b, OH), 2928, 2305, 1643 (s, C=O), 1571, 1504, 1450, 1377, 1348, 1310, 1292, 1266 (s, C–O), 1237, 1193, 1153, 1063, 1038, 969, 896, 874, 846, 804, 750, 727.

MS (EI) *m*/*z* 150 $[M]^+$, 149 $[M - H]^+$, 132 $[M - H_2O]^+$.

4.2.4. 2-Hydroxy-3-isopropyl-6-methylbenzaldehyde

Using the general procedure with 2-isopropyl-5-methylphenol (thymol) (15.02 g), the mixture was heated at reflux temperature for 3 h during which time the solution turned yellow. A yellow oil was obtained (17.32 g), which was found to contain the target compound (70% by ^{1}H NMR). A sample of the oil (1.60 g) was purified by flash column chromatography (hexane:diethyl ether 8:1). Similar fractions (TLC analysis) were collected together and volatiles were removed under reduced pressure to leave a pale green oil (1.08 g).

Yield from 1.60 g of crude product = 1.08 g, 66%.

Anal. found (Calculated for $C_{11}H_{14}O_2$)% C 74.09 (74.13), H 7.95 (7.92).

^{1}H NMR 300 MHz ($CDCl_3$) δ ppm 12.30 (s, 1H, ArO*H*), 10.29 (s, 1H, *H*C=O), 7.31 (d, 1H, Ar*H*, $^3J_{HH}$ = 8 Hz), 6.66 (d, 1H, Ar*H*, $^3J_{HH}$ = 8 Hz), 3.32 (m, 1H, C*H*Me$_2$, $^3J_{HH}$ = 7 Hz), 2.56 (s, 3H, *Me*), 1.21 (d, 6H, CH*Me*$_2$, $^3J_{HH}$ = 7 Hz).

^{13}C{^{1}H} NMR 75 MHz ($CDCl_3$) δ ppm 195.5 (H*C*=O), 160.7, 139.0, 135.1, 133.8, 121.2, 117.8 (Ar), 25.8 (*C*HMe$_2$), 22.1 (CH*Me*$_2$), 17.7 (*Me*).

IR (thin film) ν cm^{-1} 3041 (w, OH), 2963, 2875, 2579, 2361, 2343, 1896, 1821, 1633 (s, C=O), 1584, 1508, 1427, 1382, 1350, 1328, 1302, 1273 (m, C–O), 1248, 1226, 1178, 1151, 1110, 1097, 1068, 1049, 1035, 1000, 967, 923, 866, 821, 774, 735, 684, 660, 605, 595, 549.

MS (EI) *m*/*z* 178 $[M]^+$, 163 $[M - CH_3]^+$, 148 $[M - (CH_3)_2]^+$.

4.2.5. Synthesis of 2-hydroxy-3-tert-butyl-6-methylbenzaldehyde

Using the general procedure with 2-*tert*-butyl-5-methylphenol (16.43 g), the mixture was heated at reflux temperature for 1.5 h during which time the solution turned green/yellow. A yellow/orange gum was obtained (15.44 g) which was found to contain the target compound (66% by ^{1}H NMR). A sample of the solid (2.00 g) was purified by flash column chromatography (hexane:diethyl ether 4:1), to yield a yellow/green oil. The gum was also purified by distillation at 110 °C, 2 mm Hg, to yield a yellow/green oil.

Yield = 8.21 g, 43% (from distillation).

Anal. found (Calculated for $C_{12}H_{16}O_2$)% C 75.11 (74.97), H 8.42 (8.39).

^{1}H NMR 300 MHz ($CDCl_3$) δ ppm 12.72 (s, 1H, ArO*H*), 10.29 (s, 1H, *H*C=O), 7.37 (d, 1H, Ar*H*, $^3J_{HH}$ = 8 Hz), 6.64 (dd, 1H, Ar*H*, $^3J_{HH}$ = 8 Hz, $^4J_{HH}$ = 1 Hz), 2.55 (s, 3H, *Me*), 1.40 (s, 9H, C*Me*$_3$).

^{13}C{^{1}H} NMR 75 MHz ($CDCl_3$) δ ppm 195.7 (H*C*=O), 162.7, 139.6, 136.3, 134.4, 120.9, 118.2 (Ar), 34.4 (*C*Me$_3$), 29.1 (C*Me*$_3$), 17.7 (*Me*).

IR (thin film) ν cm^{-1} 3473 (b, OH), 3262, 2959, 2772, 2590, 1898, 1765, 1638 (s, C=O), 1578, 1485, 1452, 1427, 1401, 1380, 1362, 1332, 1306, 1285, 1266 (m, C–O), 1241, 1196, 1133, 1083, 1051, 1028, 969, 948, 930, 818, 794, 735, 643, 607, 595.

MS (EI) *m*/*z* 192 $[M]^+$, 177 $[M - CH_3]^+$.

4.2.6. 2-Hydroxy-3-tert-butyl-5-methylbenzaldehyde

Using the general procedure with 2-*tert*-butyl-4-methylphenol (16.43 g), the mixture was heated at reflux

temperature for 3 h during which time the solution turned orange/yellow. A yellow solid was obtained and was found to contain the target compound (67% purity by ^{1}H NMR). The solid was dissolved in pentane, concentrated and stored at −30 °C overnight to yield pale green crystals which were isolated by vacuum filtration. These were found to be the pure aldehyde. Further crops were obtained by concentration of the supernatant.

Yield = 9.70 g, 50%.

Anal. found (Calculated for $C_{12}H_{16}O_2$)% C 75.08 (74.97), 8.46 (8.39).

^{1}H NMR 300 MHz ($CDCl_3$) δ ppm 11.61 (s, 1H, ArO*H*), 9.81 (s, 1H, *H*C=O), 7.33 (d, 1H, Ar*H*, $^4J_{HH}$ = 2 Hz), 7.17 (d, 1H, Ar*H*, $^4J_{HH}$ = 2 Hz), 2.32 (s, 3H, *Me*), 1.41 (s, 9H, C*Me*$_3$).

^{13}C{^{1}H} NMR 75 MHz ($CDCl_3$) δ ppm 196.9 (H*C*=O), 159.0, 137.8, 135.3, 131.3, 128.0, 120.2 (Ar), 34.6 (*C*Me$_3$), 29.1 (C*Me*$_3$), 20.4 (*Me*).

IR (CH_2Cl_2 thin film) ν cm^{-1} 3357 (b, OH), 3002, 2964, 2868, 1649 (s, C=O), 1599, 1514, 1461, 1392, 1356, 1323, 1266 (m, C–O), 1232, 1197, 1161, 1020, 972, 932, 866, 793, 768, 747, 710.

MS (EI) *m*/*z* 192 $[M]^+$, 177 $[M - CH_3]^+$, 163 $[M - CHO]^+$.

4.3. Synthesis of Schiff base proligands

A 100 ml round bottom flask with stirrer bar was charged with the appropriate salicylaldehyde and a stoichiometric amount of the appropriate amine (racemic 2,2′-diamino-6,6′-dimethylbiphenyl for $H_2\mathbf{L}^{4-9}$ and aniline for $H\mathbf{L}^{10-13}$). The reactants were dissolved in ethanol or methanol (40–100 ml), and heated at reflux for ca. 18 h, using a condenser fitted with a drying tube containing $CaCl_2$. A precipitate generally formed during the reaction and the solid was isolated by vacuum filtration and washed with cold ethanol or methanol. All remaining volatiles were removed in vacuo.

4.3.1. $H_2\boldsymbol{L}^4$

Following the general procedure, 2-hydroxy-3,6-dimethylbenzaldehyde (2.00 g, 13.33 mmol), 2,2′-diamino-6,6′-dimethylbiphenyl (1.41 g, 6.65 mmol) and ethanol (40 ml) were used. An orange solid was obtained.

Yield = 2.44 g, 77%.

Anal. found (Calculated for $C_{32}H_{32}N_2O_2$)% C 80.69 (80.64), H 6.80 (6.77), N 6.00 (5.88).

^{1}H NMR 300 MHz ($CDCl_3$) δ ppm 13.24 (s, 2H, ArO*H*), 8.68 (s, 2H, N=C*H*), 7.33 (t, 2H, Ar*H*, $^3J_{HH}$ = 8 Hz), 7.22 (d, 2H, Ar*H*, $^3J_{HH}$ = 7 Hz), 6.99 (d, 2H, Ar*H*), 6.99 (d, 2H, Ar*H*), 6.47 (d, 2H, Ar*H*, $^3J_{HH}$ = 8 Hz), 2.26 (s, 6H, *Me*), 2.09 (s, 6H, *Me*), 2.07 (s, 6H, *Me*).

^{13}C{^{1}H} NMR 75 MHz ($CDCl_3$) δ ppm 160.5 (N=*C*H), 160.4, 147.9, 137.0, 137.0, 133.9, 132.7, 128.5, 128.3, 124.1, 119.8, 116.3, 116.2 (Ar), 19.9 (*Me*), 18.6 (*Me*), 15.4 (*Me*).

IR (CH_2Cl_2 thin film) ν cm^{-1} 3428 (b, OH), 2923, 1605 (s, N=C), 1569, 1454, 1379, 1359, 1283 (m, C–O), 1253, 1224, 1056, 1034, 985, 938, 804, 759.

MS (EI) *m*/*z* 476 $[M]^+$.

4.3.2. $H_2\boldsymbol{L}^5$

Following the general procedure, 2-hydroxy-3-methyl-6-isopropylbenzaldehyde (1.10 g, 6.17 mmol), 2,2′-diamino-6,6′-dimethylbiphenyl (0.655 g, 3.09 mmol) and ethanol (40 ml) were used. A yellow solid was obtained.

Yield = 1.37 g, 84%.

Anal. found (Calculated for $C_{36}H_{40}N_2O_2$)% C 80.83 (81.17), H 7.53 (7.57), 5.21 (5.26).

^{1}H NMR 300 MHz ($CDCl_3$) δ ppm 13.47 (s, 2H, ArO*H*), 8.89 (s, 2H, N=C*H*), 7.34 (t, 2H, Ar*H*, $^3J_{HH}$ = 8 Hz), 7.22 (d, 2H, Ar*H*, $^3J_{HH}$ = 7 Hz), 7.07 (d, 2H, Ar*H*, $^3J_{HH}$ = 8 Hz), 7.01 (d, 2H, Ar*H*, $^3J_{HH}$ = 7 Hz), 6.61 (d, 2H, Ar*H*, $^3J_{HH}$ = 8 Hz), 3.28 (m, 2H, C*H*Me$_2$, $^3J_{HH}$ = 7 Hz), 2.09 (s, 6H, *Me*), 2.06 (s, 6H, *Me*), 1.21 (d, 6H, CH*Me*$_2$, $^3J_{HH}$ = 7 Hz), 1.12 (d, 6H, CH*Me*$_2$, $^3J_{HH}$ = 7 Hz).

^{13}C{^{1}H} NMR 75 MHz ($CDCl_3$) δ ppm 160.5, 160.0 (N=*C*H), 147.8, 147.6, 137.0, 134.0, 132.9, 128.5, 128.3, 123.6, 116.2, 114.9, 114.2 (Ar), 27.9 (*C*HMe$_2$), 24.2 (CH*Me*$_2$), 23.7 (CH*Me*$_2$), 19.9 (*Me*), 15.5 (*Me*).

IR (CH_2Cl_2 thin film) ν cm^{-1} 2955, 2867, 2295, 1603 (s, N=C), 1568, 1454, 1428, 1378, 1364, 1299, 1261 (m, C–O), 1225, 1171, 1107, 1042, 983, 941, 847, 817, 798, 780, 762, 737, 649.

MS (EI) *m*/*z* 532 $[M]^+$, 517 $[M - CH_3]^+$.

4.3.3. $H_2\boldsymbol{L}^6$

Following the general procedure, 2-hydroxy-4,6-dimethylbenzaldehyde (5.00 g, 33.33 mmol), 2,2′-diamino-6,6′-dimethylbiphenyl (3.53 g, 16.65 mmol) and ethanol (100 ml) were used. An orange solid was obtained.

Yield = 6.82 g, 86%.

Anal. found (Calculated for $C_{32}H_{32}N_2O_2$)% C 79.17 (80.64), H 6.87 (6.77), N 5.52 (5.88).

^{1}H NMR 300 MHz ($CDCl_3$) δ ppm 13.16 (s, 2H, ArO*H*), 8.71 (s, 2H, N=C*H*), 7.38 (t, 2H, Ar*H*, $^3J_{HH}$ = 8 Hz), 7.25 (d, 2H, Ar*H*, $^3J_{HH}$ = 7 Hz), 7.08 (d, 2H, Ar*H*, $^3J_{HH}$ = 8 Hz), 6.50 (s, 2H, Ar*H*), 6.41 (s, 2H, Ar*H*), 2.27 (s, 6H, *Me*), 2.21 (s, 6H, *Me*), 2.08 (s, 6H, *Me*).

^{13}C{^{1}H} NMR 75 MHz ($CDCl_3$) δ ppm 162.0, 159.1 (N=*C*H), 147.2, 143.9, 139.2, 137.0, 133.1, 128.4, 128.2, 121.7, 115.7, 115.3, 114.6 (Ar), 21.6 (*Me*), 19.7 (*Me*), 18.6 (*Me*).

IR (CH_2Cl_2 thin film) ν cm^{-1} 3428 (b, OH), 2360, 1608 (s, N=C), 1558, 1453, 1356, 1302, 1268, 1229 (s, C–O), 1202, 1152, 1062, 1017, 971, 940, 836, 783, 736.

MS (EI) *m*/*z* 476 $[M]^+$.

4.3.4. H_2L^7

Following the general procedure, 2-hydroxy-3-isopropyl-6-methylbenzaldehyde (1.55 g, 8.65 mmol), 2,2′-diamino-6,6′-dimethylbiphenyl (0.91 g, 4.29 mmol) and ethanol (40 ml) were used. An orange solid was obtained.

Yield = 1.62 g, 71%.

Anal. found (Calculated for $C_{36}H_{40}N_2O_2$)% C 81.13 (81.17), H 7.68 (7.57), N 4.96 (5.26).

^{1}H NMR 300 MHz ($CDCl_3$) δ ppm 13.40 (s, 2H, ArO*H*), 8.69 (s, 2H, N=C*H*), 7.35 (t, 2H, Ar*H*, $^3J_{HH}$ = 8 Hz), 7.24 (d, 2H, Ar*H*, $^3J_{HH}$ = 7 Hz), 7.09 (d, 2H, Ar*H*, $^3J_{HH}$ = 8 Hz), 7.01 (d, 2H, Ar*H*, $^3J_{HH}$ = 8 Hz), 6.55 (d, 2H, Ar*H*, $^3J_{HH}$ = 8 Hz), 3.22 (m, 2H, C*H*Me$_2$, $^3J_{HH}$ = 7 Hz), 2.25 (s, 6H, *Me*), 2.11 (s, 6H, *Me*), 1.16 (d, 6H, CH*Me*$_2$, $^3J_{HH}$ = 7 Hz), 1.15 (d, 6H, CH*Me*$_2$, $^3J_{HH}$ = 7 Hz).

^{13}C{^{1}H} NMR 75 MHz ($CDCl_3$) δ ppm 160.5 (N=*C*H), 159.5, 147.9, 136.9, 136.7, 134.4, 132.6, 129.3, 128.4, 128.1, 119.8, 116.3, 116.0 (Ar), 26.0 (*C*HMe$_2$), 22.3 (CH*Me*$_2$), 22.1 (CH*Me*$_2$), 19.8 (*Me*), 18.4 (*Me*).

IR (CH_2Cl_2 thin film) ν cm^{-1} 3476 (b, OH), 2960, 2870, 1602 (s, N=C), 1569, 1438, 1380, 1360, 1300, 1274 (m, C–O), 1247, 1219, 1152, 1108, 1067, 1048, 987, 941, 813, 771, 740.

MS (EI) *m*/*z* 532 [M]$^+$.

4.3.5. H_2L^8

Following the general procedure, 2-hydroxy-3-*tert*-butyl-6-methylbenzaldehyde (1.36 g, 7.08 mmol), 2,2′-diamino-6,6′-dimethylbiphenyl (0.74 g, 3.49 mmol) and ethanol (40 ml) were used. An orange solid was obtained.

Yield = 1.56 g, 80%.

Anal. found (Calculated for $C_{38}H_{44}N_2O_2$)% C 81.38 (81.39), H 7.87 (7.91), N 4.99 (5.00).

^{1}H NMR 300 MHz ($CDCl_3$) δ ppm 13.87 (s, 2H, ArO*H*), 8.71 (s, 2H, N=C*H*), 7.34 (t, 2H, Ar*H*, $^3J_{HH}$ = 8 Hz), 7.23 (d, 2H, Ar*H*, $^3J_{HH}$ = 7 Hz), 7.12 (d, 2H, Ar*H*, $^3J_{HH}$ = 8 Hz), 7.04 (d, 2H, Ar*H*, $^3J_{HH}$ = 8 Hz), 6.48 (dd, 2H, Ar*H*, $^3J_{HH}$ = 8 Hz, $^4J_{HH}$ = 1 Hz), 2.23 (s, 6H, *Me*), 2.11 (s, 6H, *Me*), 1.30 (s, 18H, C*Me*$_3$).

^{13}C{^{1}H} NMR 75 MHz ($CDCl_3$) δ ppm 161.6, 159.9 (N=*C*H), 147.3, 137.2, 137.0, 135.5, 133.0, 129.9, 128.3, 128.2, 119.3, 116.7, 115.4 (Ar), 34.4 (*C*Me$_3$), 29.1 (C*Me*$_3$), 19.8 (*Me*), 18.4 (*Me*).

IR (CH_2Cl_2 thin film) ν cm^{-1} 3426 (b, OH), 2957, 2871, 2361, 2094, 1643, 1601 (s, N=C), 1568, 1484, 1436, 1361, 1288, 1266 (m, C–O), 1236, 1197, 1136, 1051, 1018, 976, 942, 813, 792, 770, 739.

MS (EI) *m*/*z* 560 [M]$^+$, 545 [M − CH$_3$]$^+$.

4.3.6. H_2L^9

Following the general procedure, 2-hydroxy-3-*tert*-butyl-5-methylbenzaldehyde (2.00 g, 10.40 mmol), 2,2′-diamino-6,6′-dimethylbiphenyl (1.08 g, 5.09 mmol) and ethanol (40 ml) were used. An orange solid was obtained.

Yield = 2.52 g, 88%.

Anal. found (Calculated for $C_{38}H_{44}N_2O_2$)% C 81.33 (81.39), H 7.97 (7.91), N 5.04 (5.00).

^{1}H NMR 300 MHz ($CDCl_3$) δ ppm 12.84 (s, 2H, ArO*H*), 8.37 (s, 2H, N=C*H*), 7.32 (t, 2H, Ar*H*, $^3J_{HH}$ = 8 Hz), 7.21 (d, 2H, Ar*H*, $^3J_{HH}$ = 8 Hz), 7.07 (d, 2H, Ar*H*, $^4J_{HH}$ = 2 Hz), 7.02 (2H, Ar*H*, $^3J_{HH}$ = 8 Hz), 6.85 (d, 2H, Ar*H*, $^4J_{HH}$ = 2 Hz), 2.23 (s, 6H, *Me*), 2.09 (s, 6H, *Me*), 1.32 (s, 18H, C*Me*$_3$).

^{13}C{^{1}H} NMR 75 MHz ($CDCl_3$) δ ppm 162.1 (N=*C*H), 158.2, 146.9, 137.0, 136.9, 133.2, 130.8, 130.0, 128.2, 128.1, 126.2, 118.5, 115.1 (Ar), 34.6 (*C*Me$_3$), 29.1 (C*Me*$_3$), 20.5 (*Me*), 19.7 (*Me*).

IR (CH_2Cl_2 thin film) ν cm^{-1} 3357 (b, OH), 2957, 2916, 2864, 2740, 1619 (s, N=C), 1568, 1462, 1438, 1390, 1384, 1359, 1318, 1266 (w, C–O), 1230, 1210, 1163, 1104, 1024, 980, 948, 927, 861, 813, 786, 772, 746, 688.

MS (EI) *m*/*z* 560 [M]$^+$, 545 [M − CH$_3$]$^+$.

4.3.7. HL^{10}

Following the general procedure, 2-hydroxy-3-*tert*-butyl-6-methylbenzaldehyde (1.50 g, 7.81 mmol), aniline (0.73 g, 7.85 mmol) and methanol (40 ml) were used. The solution was kept at −30 °C before filtration and an orange solid was obtained.

Yield = 1.75 g, 84%.

Anal. found (Calculated for $C_{18}H_{21}NO$)% C 80.81 (80.86), H 7.99 (7.92), N 5.24 (5.24).

^{1}H NMR 300 MHz ($CDCl_3$) δ ppm 14.71 (s, 1H, ArO*H*), 8.98 (s, 1H, N=C*H*), 7.44 (t, 2H, Ar*H*, $^3J_{HH}$ = 8 Hz), 7.31–7.27 (m, 4H, Ar*H*), 6.65 (d, 1H, Ar*H*, $^3J_{HH}$ = 8 Hz), 2.51 (s, 3H, *Me*), 1.47 (s, 9H, C*Me*$_3$).

^{13}C{^{1}H} NMR 75 MHz ($CDCl_3$) δ ppm 162.2, 161.0 (N=*C*H), 148.7, 137.3, 135.8, 130.5, 129.3, 126.5, 121.2, 120.0, 116.8 (Ar), 34.6 (*C*Me$_3$), 29.3 (C*Me*$_3$), 18.8 (*Me*).

IR (CH_2Cl_2 thin film) ν cm^{-1} 3383 (b, OH), 2999, 2941, 2552 (b, OH), 1606 (s, N=C), 1580, 1481, 1457, 1434, 1384, 1360, 1301, 1286 (m, C–O), 1190, 1137, 1078, 1025, 978, 966, 927, 904, 851, 813, 777, 758, 731, 693.

MS (EI) *m*/*z* 267 [M]$^+$, 252 [M − CH$_3$]$^+$, 250 [M − OH]$^+$.

4.3.8. Synthesis of HL^{11} [16]

Following the general procedure, 3-*tert*-butyl-2-hydroxy-5-methylbenzaldehyde (1.87 g, 9.74 mmol), aniline (0.91 g, 9.78 mmol) and methanol (40 ml) were used. The solution was kept at −30 °C before filtration and an orange solid was obtained.

Yield = 2.05 g, 79%.

Anal. found (Calculated for $C_{18}H_{21}NO$)% C 80.89 (80.86), H 7.94 (7.92), N 5.27 (5.24).

^{1}H NMR 300 MHz ($CDCl_3$) δ ppm 13.69 (s, 1H, ArO*H*), 8.56 (s, 1H, N=C*H*), 7.40 (t, 2H, Ar*H*, $^3J_{HH}$ = 8 Hz), 7.26 (d, 2H, Ar*H*, $^3J_{HH}$ = 8 Hz), 7.25 (t, 1H, Ar*H*), 7.19 (d, 1H, Ar*H*, $^4J_{HH}$ = 2 Hz), 7.03 (d, 1H, Ar*H*, $^4J_{HH}$ = 2 Hz), 2.30 (s, 3H, *Me*), 1.46 (s, 9H, C*Me*$_3$).

^{13}C{^{1}H} NMR 75 MHz ($CDCl_3$) δ ppm 163.2 (N=*C*H), 158.2, 148.5, 137.3, 131.4, 130.3, 129.2, 126.9, 126.5, 121.0, 118.6 (Ar), 34.7 (*C*Me$_3$), 29.3 (C*Me*$_3$), 20.6 (*Me*).

IR (CH_2Cl_2 thin film) ν cm^{-1} 2957, 2913, 2760, 1941, 1764, 1727, 1618 (s, N=C), 1581, 1485, 1440, 1390, 1361, 1320, 1267 (s, C–O), 1236, 1206, 1164, 1076, 1027, 981, 930, 903, 862, 801, 782, 759, 691.

MS (EI) *m*/*z* 267 $[M]^+$, 252 $[M - CH_3]^+$, 250 $[M - OH]^+$.

4.3.9. *HL*[12]

Following the general procedure, 2-hydroxy-3,6-dimethylbenzaldehyde (0.53 g, 3.53 mmol), aniline (0.33 g, 3.55 mmol) and methanol (40 ml) were used. The solution was kept at −30 °C before filtration and an orange solid was obtained.

Yield = 0.72 g, 91%.

Anal. found (Calculated for $C_{15}H_{15}NO$)% C 79.47 (79.97), H 6.73 (6.71), N 6.04 (6.22).

^{1}H NMR 300 MHz ($CDCl_3$) δ ppm 14.28 (s, 1H, ArO*H*), 8.85 (s, 1H, N=C*H*), 7.32 (t, 2H, Ar*H*, $^3J_{HH}$ = 8 Hz), 7.18 (t, 1H, Ar*H*), 7.17 (d, 2H, Ar*H*), 7.02 (d, 1H, Ar*H*, $^3J_{HH}$ = 7 Hz), 6.51 (d, 1H, ArH_c, $^3J_{HH}$ = 8 Hz), 2.39 (s, 3H, *Me*), 2.18 (s, 3H, *Me*).

^{13}C{^{1}H} NMR 75 MHz ($CDCl_3$) δ ppm 160.5, 160.5 (N=*C*H), 148.6, 136.9, 134.2, 129.3, 126.5, 124.3, 121.1, 120.2, 116.2 (Ar), 18.7 (*Me*), 15.3 (*Me*).

IR (CH_2Cl_2 thin film) ν cm^{-1} 3033, 3004, 2949, 2924, 2734, 2672, 1940, 1867, 1609 (s, N=C), 1578, 1503, 1484, 1459, 1434, 1380, 1362, 1308, 1283 (s, C–O), 1253, 1201, 1171, 1157, 1076, 1054, 1034, 986, 943, 905, 852, 806, 770, 754, 738, 714, 692, 593, 559.

MS (EI) *m*/*z* 225 $[M]^+$, 208 $[M - OH]^+$.

4.3.10. *HL*[13]

Following the general procedure, 2-hydroxy-3,5-dimethylbenzaldehyde (0.978 g, 6.52 mmol), aniline (0.61 g, 6.56 mmol) and methanol (40 ml) were used. Evaporation of volatiles gave an orange oil.

Yield = 1.28 g, 87%.

Anal. found (Calculated for $C_{15}H_{15}NO$)% C 79.88 (79.97), H 6.73 (6.71), N 6.10 (6.22).

^{1}H NMR 300 MHz ($CDCl_3$) δ ppm 13.37 (s, 1H, ArO*H*), 8.56 (s, 1H, N=C*H*), 7.43 (t, 2H, Ar*H*, $^3J_{HH}$ = 8 Hz), 7.28 (t, 1H, Ar*H*), 7.28 (d, 2H, Ar*H*), 7.09 (s,1H, Ar*H*), 7.03 (s, 1H, Ar*H*), 2.32 (s, 3H, *Me*), 2.31 (s, 3H, *Me*).

^{13}C{^{1}H} NMR 75 MHz ($CDCl_3$) δ ppm 162.6 (N=*C*H), 157.1, 148.5, 135.1, 129.7, 129.2, 127.4, 126.5, 125.7, 121.0, 117.9 (Ar), 20.2 (Me), 15.3 (Me).

IR (thin film) ν cm^{-1} 3030, 2982, 2919, 2771, 1944, 1752, 1621 (s, N=C), 1585, 1490, 1474, 1435, 1380, 1364, 1324, 1280, 1267 (s, C–O), 1205, 1167, 1076, 1049, 1025, 976, 961, 906, 862, 810, 781, 766, 747, 708, 692.

MS (EI) *m*/*z* 225 $[M]^+$, 210 $[M - CH_3]^+$.

4.4. *Na$_2$L^n·THF$_x$ and NaL^n·THF$_x$*

A Schlenk vessel with stirrer bar was charged with the appropriate proligand (0.5–1.5 g), and a twofold excess of NaH·THF (40 ml) was added and the solution stirred overnight under a vented inert atmosphere. The stirring was stopped and unreacted NaH allowed to settle before filtering the solution through a cannula. THF was removed in vacuo to yield a solid. The product was analysed by ^{1}H NMR spectroscopy in d^5-pyridine and the THF content thereby estimated.

4.5. *Zirconium alkyl complexes*

4.5.1. *[ZrL^4(CH$_2$Ph)$_2$]*

A Schlenk vessel with stirrer bar was charged with H_2L^4 (247 mg, 0.52 mmol) and $[Zr(CH_2Ph)_2]$ (250 mg, 0.55 mmol). The vessel was placed in a dry ice/acetone bath at −78 °C and dichloromethane (30 ml) was added. This was stirred for 30 min and then filtered at −78 °C, followed by removal of solvent under reduced pressure. The orange solid obtained was then washed with acetonitrile, filtered and dried in vacuo.

Yield = 266 mg, 68%.

Anal. found (Calculated for $C_{46}H_{44}N_2O_2Zr$)% C 73.56 (73.86), H 5.60 (5.93), N 3.85 (3.74).

^{1}H NMR 400 MHz (CD_2Cl_2) δ ppm 8.14 (s, 2H, N=C*H*), 7.24 (d, 2H, Ar*H*, $^3J_{HH}$ = 8 Hz), 7.06 (t, 2H, Ar*H*, $^3J_{HH}$ = 8 Hz), 7.02 (d, 2H, Ar*H*, $^3J_{HH}$ = 7 Hz), 6.96 (t, 4H, Ar*H*, $^3J_{HH}$ = 8 Hz), 6.79 (t, 2H, Ar*H*, $^3J_{HH}$ = 7 Hz), 6.64 (d, 4H, Ar*H*, $^3J_{HH}$ = 7 Hz), 6.55 (d, 2H, Ar*H*, $^3J_{HH}$ = 7 Hz), 6.53 (d, 2H, Ar*H*, $^3J_{HH}$ = 7 Hz), 2.34 (s, 6H, *Me*), 2.25 (s, 6H, *Me*), 2.09 (s, 6H, *Me*), 1.89 (d, 2H, C*H*$_2$Ph, $^2J_{HH}$ = 8 Hz), 1.61 (d, 2H, C*H*$_2$Ph, $^2J_{HH}$ = 8 Hz).

^{13}C{^{1}H} NMR 100 MHz (CD_2Cl_2) δ ppm 165.7 (N=*C*H), 161.9, 150.4, 144.1, 138.8, 136.7, 136.0, 131.3, 128.4, 128.2, 127.9, 127.7, 126.0, 120.9, 120.0, 120.0, 120.0 (*Ar*), 60.3 (*C*$_2$Ph), 19.8 (*Me*), 19.2 (*Me*), 16.9 (*Me*).

IR (Nujol) ν cm^{-1} 2727, 2284, 1600 (m, N=C), 1562, 1297 (m, C–O), 1249, 1219, 1140, 1062, 1027, 993, 968, 940, 915, 876, 815, 748, 720, 697, 646.

MS (CI) *m*/*z* 747 $[M - H]^+$, 733 $[M - CH_3]^+$, 718 $[M - (CH_3)_2]^+$, 657 $[M - CH_2Ph]^+$.

4.5.2. *[ZrL^5(CH$_2$Ph)$_2$]*

A Schlenk vessel with stirrer bar was charged with H_2L^5 (449 mg, 0.84 mmol) and $[Zr(CH_2Ph)_4]$ (402 mg, 0.88 mmol). The vessel was placed in an acetone/dry

ice bath at −78 °C and acetonitrile (20 ml) added. This was transferred to an ice bath at 0 °C and allowed to stir for 20 min. An orange precipitate formed and was isolated by filtration at 0 °C, followed by washing with cold acetonitrile. The orange solid was dried in vacuo.

Yield = 486 mg, 72%.

Anal. found (Calculated for $C_{50}H_{52}N_2O_2Zr$)% C 72.28 (74.68), H 6.44 (6.52), N 3.34 (3.48).

^{1}H NMR 400 MHz (CD_2Cl_2) δ ppm 8.26 (s, 2H, N=C*H*), 7.33 (d, 2H, Ar*H*, $^3J_{HH}$ = 8 Hz), 7.06 (t, 2H, Ar*H*, $^3J_{HH}$ = 8 Hz), 7.01 (d, 2H, Ar*H*, $^3J_{HH}$ = 7 Hz), 6.95 (t, 4H, Ar*H*, $^3J_{HH}$ = 8 Hz), 6.80 (t, 2H, Ar*H*, $^3J_{HH}$ = 7 Hz), 6.68 (d, 2H, Ar*H*, $^3J_{HH}$ = 8 Hz), 6.63 (d, 4H, Ar*H*, $^3J_{HH}$ = 7 Hz), 6.42 (d, 2H, Ar*H*, $^3J_{HH}$ = 7 Hz), 3.07 (m, 2H, C*H*Me$_2$, $^3J_{HH}$ = 7 Hz), 2.33 (s, 6H, *Me*), 2.07 (s, 6H, *Me*), 1.89 (d, 2H, C*H*$_2$Ph, $^2J_{HH}$ = 8 Hz), 1.49 (d, 2H, C*H*$_2$Ph, $^2J_{HH}$ = 8 Hz), 1.26 (d, 2H, CH*Me*$_2$, $^3J_{HH}$ = 7 Hz), 1.11 (d, 2H, CH*Me*$_2$, $^3J_{HH}$ = 7 Hz).

^{13}C{^{1}H} 75 MHz NMR ($CDCl_3$) δ 165.4 (N=*C*H), 161.9, 150.9, 149.6, 144.5, 136.9, 136.4, 131.3, 128.6, 128.3, 128.1, 128.0, 125.7, 121.2, 120.3, 118.5, 114.9 (*Ar*), 60.4 (C*H*$_2$Ph), 28.7 (*C*HMe$_2$), 24.5 (CH*Me*$_2$), 23.8 (CH*Me*$_2$), 20.0 (*Me*), 17.3 (*Me*).

IR (Nujol) ν cm^{-1} 2725, 2359, 1593 (s, N=C), 1580, 1559, 1405, 1316, 1304, 1278 (m, C–O), 1256, 1216, 1176, 1157, 1102, 1044, 1026, 997, 970, 939, 911, 872, 816, 801, 778, 761, 754, 742, 719, 696, 647.

MS (EI) *m*/*z* 622 [M$^+$ − $(CH_2Ph)_2$].

4.5.3. [Zr**L**^{6}$(CH_2Ph)_2$]

The complex was synthesised analogously to [Zr**L**^{5}$(CH_2Ph)_2$] using H_2**L**^{6} (279 mg, 0.59 mmol) and [Zr$(CH_2Ph)_4$] (275 mg, 0.60 mmol). A pale orange solid was obtained.

Yield = 274 mg, 62%.

Anal. found (Calculated for $C_{44}H_{40}N_2O_2Zr$)% C 71.30 (73.40), 5.49 (5.60), N 3.39 (3.89).

^{1}H NMR 400 MHz (CD_2Cl_2) δ ppm 8.15 (s, 2H, N=C*H*), 7.05 (t, 2H, Ar*H*, $^3J_{HH}$ = 8 Hz), 7.03 (d, 2H, Ar*H*, $^3J_{HH}$ = 8 Hz), 7.00 (t, 4H, Ar*H*, $^3J_{HH}$ = 8 Hz), 6.84 (t, 2H, Ar*H*, $^3J_{HH}$ = 7 Hz), 6.64 (d, 2H, Ar*H*, $^3J_{HH}$ = 7 Hz), 6.52 (s, 2H, Ar*H*), 6.49 (s, 2H, Ar*H*), 6.28 (dd, 2H, Ar*H*, $^3J_{HH}$ = 7 Hz, $^4J_{HH}$ = 2 Hz), 2.33 (s, 6H, *Me*), 2.26 (s, 6H, *Me*), 2.05 (s, 6H, *Me*), 1.68 (d, 2H, C*H*$_2$Ph, $^2J_{HH}$ = 8 Hz), 1.27 (d, 2H, C*H*$_2$Ph, $^2J_{HH}$ = 8 Hz).

^{13}C{^{1}H} NMR 100 MHz (CD_2Cl_2) δ ppm 164.7 (N=*C*H), 163.7, 150.1, 147.3, 144.0, 141.1, 136.6, 131.1, 128.8, 128.2, 128.0, 127.9, 122.2, 121.1, 120.2, 118.2, 117.8 (*Ar*), 59.6 (*C*$_2$Ph), 21.9 (*Me*), 19.8 (*Me*), 19.3 (*Me*).

IR (Nujol) ν cm^{-1} 2726, 2361, 1592 (m, N=C), 1533, 1410, 1348, 1308, 1228, 1203 (w, C–O), 1161, 1073, 1028, 976, 938, 837, 782, 722, 696, 647.

MS (EI): did not produce assignable peaks.

4.5.4. [Zr**L**^{7}$(CH_2Ph)_2$]

The complex was synthesised in an analogous manner to [Zr**L**^{5}$(CH_2Ph)_2$], using H_2**L**^{7} (366 mg, 0.69 mmol) and [Zr$(CH_2Ph)_4$] (313 mg, 0.69 mmol). The complex was obtained as an orange solid.

Yield = 396 mg, 71%.

Anal. found (Calculated for $C_{48}H_{48}N_2O_2Zr$)% C 72.74 (74.28), H 6.47 (6.23), N 3.38 (3.61).

^{1}H NMR 500 MHz (CD_2Cl_2) δ ppm 8.06 (s, 2H, N=C*H*), 7.26 (d, 2H, Ar*H*, $^3J_{HH}$ = 8 Hz), 7.03 (t, 2H, Ar*H*, $^3J_{HH}$ = 8 Hz), 6.99 (d, 2H, Ar*H*, $^3J_{HH}$ = 7 Hz), 6.92 (t, 4H, Ar*H*, $^3J_{HH}$ = 8 Hz), 6.77 (t, 2H, Ar*H*, $^3J_{HH}$ = 7 Hz), 6.59 (d, 2H, Ar*H*, $^3J_{HH}$ = 8 Hz), 6.55 (d, 2H, Ar*H*, $^3J_{HH}$ = 7 Hz), 6.54 (d, 4H, Ar*H*, $^3J_{HH}$ = 8 Hz), 3.57 (m, 2H, C*H*Me$_2$, $^3J_{HH}$ = 7 Hz), 2.22 (s, 6H, *Me*), 2.07 (s, 6H, *Me*), 1.77 (d, 2H, C*H*$_2$Ph, $^2J_{HH}$ = 8 Hz), 1.51 (d, 2H, C*H*$_2$Ph, $^2J_{HH}$ = 8 Hz), 1.36 (d, 6H, CH*Me*$_2$, $^3J_{HH}$ = 7 Hz), 1.16 (d, 6H, CH*Me*$_2$, $^3J_{HH}$ = 7 Hz).

^{13}C{^{1}H} NMR 100 MHz (CD_2Cl_2) δ ppm 165.6 (N=*C*H), 160.4, 150.5, 144.0, 138.6, 136.8, 136.4, 131.5, 131.5, 128.4, 128.0, 127.8, 127.5, 120.9, 120.4, 120.2, 120.0 (*Ar*), 60.1 (*C*$_2$Ph), 26.2 (*C*HMe$_2$), 23.9 (CH*Me*$_2$), 21.9 (CH*Me*$_2$), 19.9 (*Me*), 19.2 (*Me*).

IR (Nujol) ν cm^{-1} 2726, 2362, 1600 (s, N=C), 1559, 1406, 1365, 1353, 1307, 1282 (m, C–O), 1242, 1210, 1171, 1149, 1100, 1056, 1027, 1000, 964, 940, 901, 850, 810, 780, 742, 697, 648, 611.

MS (EI) *m*/*z* 803 [M]$^+$, 621 [M − $(CH_2Ph)_2$]$^+$.

4.5.5. [Zr**L**$_2^{10}$$(CH_2Ph)_2$]

The complex was synthesised in an analogous manner to [Zr**L**^{4}$(CH_2Ph)_2$] using H**L**^{10} (450 mg, 1.68 mol) and [Zr$(CH_2Ph)_4$] (383 mg, 0.84 mol). An orange/red solid was obtained.

Yield = 360 mg, 53%.

Anal. found (Calculated for $C_{50}H_{54}N_2O_2Zr$)% C 73.99 (74.49), H 6.52 (6.75), N 3.02 (3.47).

^{1}H NMR 400 MHz (d_6-benzene) δ ppm 8.33 (s, 2H, N=C*H*), 7.35 (d, 2H, Ar*H*, $^3J_{HH}$ = 8 Hz), 7.13 (d, 4H, Ar*H*, $^3J_{HH}$ = 8 Hz), 7.05 (t, 4H, Ar*H*, $^3J_{HH}$ = 7 Hz), 7.03 (t, 2H, Ar*H*, $^3J_{HH}$ = 8 Hz), 6.83 (t, 4H, Ar*H*, $^3J_{HH}$ = 7 Hz), 6.78 (t, 2H, Ar*H*, $^3J_{HH}$ = 7 Hz), 6.74 (d, 4H, Ar*H*, $^3J_{HH}$ = 7 Hz), 6.52 (d, 2H, Ar*H*, $^3J_{HH}$ = 8 Hz), 2.98 (d, 2H, C*H*$_2$Ph, $^2J_{HH}$ = 10 Hz), 2.88 (d, 2H, C*H*$_2$Ph, $^2J_{HH}$ = 10 Hz), 1.93 (s, 6H, *Me*), 1.51 (s, 18H, C*Me*$_3$).

^{13}C{^{1}H} NMR 100 MHz (d_6-benzene) δ ppm 167.0 (N=*C*H), 161.8, 153.3, 147.4, 139.9, 137.8, 133.3, 128.7, 128.2, 127.5, 126.3, 123.2, 123.0, 121.3, 120.7 (*Ar*), 69.2 (*C*$_2$Ph), 35.0 (*C*Me$_3$), 30.0 (C*Me*$_3$), 19.1 (*Me*).

IR (Nujol) ν cm^{-1} 2360, 2341, 1580 (m, N=C), 1558, 1487, 1404, 1298 (s, C–O), 1266, 1205, 1186, 1136, 1056, 1028, 979, 964, 907, 852, 815, 768, 744, 727, 697, 668, 639.

MS (EI) *m/z* 728 $[M - C_6H_5]^+$, 714 $[M - CH_2Ph]^+$, 651 $[M - (C_6H_5)_2]^+$, 623 $[M - (CH_2Ph)_2]^+$.

4.5.6. $[Zr\mathbf{L}^4(CH_2Bu^t)_2]$

A Schlenk vessel with stirrer bar was charged with $H_2\mathbf{L}^4$ (360 mg, 0.76 mmol) and $[Zr(CH_2CMe_3)_4]$ (284 mg, 0.76 mmol). This was cooled to −78 °C and dichloromethane (30 ml) added, with stirring of the solution. The solution was allowed to warm to room temperature and stirring was continued for a further 30 min, during which time the solution turned from yellow to orange. Removal of volatiles under reduced pressure yielded an orange/yellow solid. This was dissolved in pentane and the solution was filtered, concentrated and kept at −30 °C overnight to yield a yellow precipitate, which was isolated by filtration and dried in vacuo.

Yield = 226 mg, 42%.

Anal. found (Calculated for $C_{42}H_{52}N_2O_2Zr$)% C 68.98 (71.24), H 6.99 (7.40), N 4.07 (3.96).

^{1}H NMR 400 MHz (d_6-benzene) δ ppm 8.18 (s, 2H, N=C*H*), 7.15 (d, 2H, Ar*H*, $^3J_{HH}$ = 8 Hz), 7.07 (d, 2H, Ar*H*, $^3J_{HH}$ = 7 Hz), 6.77 (t, 2H, Ar*H*, $^3J_{HH}$ = 8 Hz), 6.49 (d, 2H, Ar*H*, $^3J_{HH}$ = 8 Hz), 6.32 (d, 2H, Ar*H*, $^3J_{HH}$ = 7 Hz), 2.62 (s, 6H, *Me*), 1.91 (s, 6H, *Me*), 1.89 (s, 6H, *Me*), 1.88 (d, 2H, C*H*$_2$CMe$_3$, $^2J_{HH}$ = 13 Hz), 1.59 (d, 2H, C*H*$_2$CMe$_3$, $^2J_{HH}$ = 13 Hz), 1.37 (s, 18H, CH$_2$C*Me*$_3$).

^{13}C{^{1}H} NMR 100 MHz (d_6-benzene) δ ppm 168.1 (N=*C*H), 162.7, 151.4, 138.0, 136.8, 136.7, 132.1, 128.1, 127.6, 127.1, 120.2, 120.0, 120.0 (*Ar*), 87.2 (*C*$_2$CMe$_3$), 35.6 (CH$_2$*C*Me$_3$), 35.1 (CH$_2$ C*Me*$_3$), 20.0 (*Me*), 18.8 (*Me*), 17.2 (*Me*).

IR (Nujol) ν cm^{-1} 2728, 2360, 1602 (s, N=C), 1561, 1400, 1322, 1302 (s, C–O), 1258, 1216, 1143, 1096, 1062, 1041, 993, 975, 938, 891, 803, 767, 747, 720, 669, 646, 600, 554.

MS (EI) *m/z* 1414 $[M_2]^+$, 1343 $[M_2 - CH_2CMe_3]^+$, 651 $[M - Me_2CH_2]^+$, 636 $[M - CH_2CMe_3]^+$.

4.6. Synthesis of zirconium chloride complexes

A Schlenk vessel with stirrer bar was charged with the sodium salt of the appropriate ligand (0.5–1.2 g) and a slight excess of $[ZrCl_4(THF)_2]$. The vessel was cooled to −78 °C and THF (40 ml) added. The solution was allowed to warm to room temperature and stirred for 20 h, during which time a precipitate formed and the solution turned usually turned from yellow to orange. Stirring was ceased and the precipitate allowed to settle before filtering the solution through a cannula. The solvent was then removed under reduced pressure to give an orange/yellow solid. The solid was then dissolved in dichloromethane and filtered, followed by removal of the solvent under reduced pressure. The solid obtained was then sublimated along a horizontal glass tube at 250–350 °C, 10^{-6} mm Hg, to yield the product.

4.6.1. $[Zr\mathbf{L}^1Cl_2]$

Following the general method, $Na_2\mathbf{L}^1\cdot THF_{0.48}$ (700 mg, 1.26 mmol) and $[ZrCl_4(THF)_2]$ (487 mg, 1.29 mmol) were used.

Yield = 722 mg, 90%.

Anal. found (Calculated for $C_{32}H_{30}Cl_2N_2O_2Zr$)% C 59.99 (60.36), H 4.72 (4.75), N 4.26 (4.40).

^{1}H NMR 300 MHz (CD_2Cl_2) δ ppm 8.21 (s, 2H, N=C*H*), 7.30 (s, 2H, Ar*H*), 7.27 (t, 2H, Ar*H*, $^3J_{HH}$ = 8 Hz), 7.20 (d, 2H, ArH_j, $^3J_{HH}$ = 7 Hz), 7.07 (s, 2H, Ar*H*), 6.98 (d, 2H, ArH_l, $^3J_{HH}$ = 7 Hz), 2.29 (s, 6H, *Me*), 2.26 (s, 6H, *Me*), 2.05 (s, 6H, *Me*).

^{13}C{^{1}H} NMR 75 MHz (CD_2Cl_2) δ ppm 169.7 (N=*C*H), 158.0, 149.3, 139.4, 137.9, 132.0, 130.7, 129.7, 129.7, 129.2, 128.8, 127.3, 122.1 (Ar), 20.2 (*Me*), 19.8 (*Me*), 15.8 (*Me*).

IR (Nujol) ν cm^{-1} 2729, 1614 (s, N=C), 1593, 1556, 1288, 1263 (s, C–O), 1218, 1171, 1160, 1105, 1063, 1016, 980, 961, 942, 902, 860, 851, 836, 817, 791, 777, 756, 736, 627.

MS (EI) *m/z* 635 $[M]^+$, 600 $[M - Cl]^+$, 585 [M − (Cl and Me)]$^+$, 530 [M − {(Cl)$_2$ and Me}]$^+$.

4.6.2. $[Zr\mathbf{L}^2Cl_2]$

Following the general method, $Na_2\mathbf{L}^2\cdot THF_{0.88}$ (800 mg, 1.25 mmol) and $[ZrCl_4(THF)_2]$ (523 mg, 1.38 mmol) were used.

Yield = 596 mg, 71%.

Anal. found (Calculated for $C_{34}H_{34}Cl_2N_2O_2Zr$)% C 61.42 (61.43), H 4.97 (5.16), N 3.86 (4.21).

^{1}H NMR 300 MHz (CD_2Cl_2) δ ppm 8.22 (s, 2H, N=C*H*), 7.51 (dd, 2H, Ar*H*, $^3J_{HH}$ = 7 Hz, $^4J_{HH}$ = 2 Hz), 7.26 (dd, 2H, Ar*H*), 7.26 (t, 2H, Ar*H*, $^3J_{HH}$ = 8 Hz), 7.19 (d, 2H, Ar*H*, $^3J_{HH}$ = 7 Hz), 7.03 (d, 2H, Ar*H*, $^3J_{HH}$ = 7 Hz), 6.96 (t, 2H, Ar*H*, $^3J_{HH}$ = 8 Hz), 3.37 (m, 2H, C*H*Me$_2$, $^3J_{HH}$ = 7 Hz), 2.07 (s, 6H, *Me*), 1.32 (d, 6H, CH*Me*$_2$, $^3J_{HH}$ = 7 Hz), 1.27 (d, 6H, $^3J_{HH}$ = 7 Hz).

^{13}C{^{1}H} NMR 75 MHz (CD_2Cl_2) δ ppm 170.0 (N=*C*H), 159.3, 149.1, 138.1, 137.9, 134.1, 132.4, 130.9, 129.2, 128.7, 122.5, 121.8, 120.4 (*Ar*), 28.1 (*C*HMe$_2$), 22.1 (CH*Me*$_2$), 21.9 (CH*Me*$_2$), 19.8 (*Me*).

IR (Nujol) ν cm^{-1} 1599 (s, N=C), 1553, 1320, 1278 (m, C–O), 1239, 1206, 1150, 1104, 1055, 1017, 984, 943, 891, 857, 806, 770, 751, 738, 710, 653, 579.

MS (EI) *m/z* 663 $[M]^+$, 628 $[M - Cl]^+$, 613 [M − (Cl and Me)]$^+$, 593 $[M - (Cl)_2]^+$.

4.6.3. $[Zr\mathbf{L}^3Cl_2]$

Following the general method, $Na_2\mathbf{L}^3\cdot THF_{0.48}$ (800 mg, 1.31 mmol) and $[ZrCl_4(THF)_2]$ (508 mg, 1.35 mmol) were used.

Yield = 634 mg, 70%.

Anal. found (Calculated for $C_{36}H_{38}Cl_2N_2O_2Zr$)% C 61.72 (62.41), 5.37 (5.53), N 3.88 (4.04).

^{1}H NMR 300 MHz (CD_2Cl_2) δ ppm 8.32 (s, 2H, N=C*H*), 7.67 (dd, 2H, Ar*H*, $^3J_{HH}$ = 9 Hz, $^4J_{HH}$ = 3 Hz),

7.44 (d, 2H, Ar*H*, $^4J_{HH}$ = 2 Hz), 7.32 (t, 2H, Ar*H*, $^3J_{HH}$ = 8 Hz), 7.26 (dd, 2H, Ar*H*, $^3J_{HH}$ = 8 Hz, $^4J_{HH}$ = 1 Hz), 7.00 (dd, 2H, Ar*H*, $^3J_{HH}$ = 8 Hz, $^4J_{HH}$ = 1 Hz), 6.86, (d, 2H, Ar*H*, $^3J_{HH}$ = 9 Hz), 2.07 (s, 6H, *Me*), 1.34 (s, 18H, C*Me*$_3$).

^{13}C{^{1}H} NMR 75 Mhz (CD_2Cl_2) δ ppm 169.8 (N=*C*H), 159.4, 149.2, 143.7, 138.1, 135.6, 131.2, 130.6, 129.5, 129.0, 122.5, 122.3, 118.1 (*Ar*), 34.2 (*C*Me$_3$), 31.1 (C*Me*$_3$), 19.8 (*Me*).

IR (Nujol) ν cm^{-1} 1614 (s, N=C), 1590, 1543, 1362, 1312, 1298, 1260 (s, C–O), 1209, 1184, 1151, 1143, 1098, 1026, 992, 982, 954, 895, 881, 838, 790, 776, 762, 738, 722, 704, 680, 667, 616.

MS (EI) *m*/*z* 692 [M]$^+$, 677 [M − CH$_3$]$^+$, 657 [M − Cl]$^+$, 622 [M − (Cl)$_2$]$^+$.

4.6.4. [Zr**L**^{4}Cl$_2$]

Following the general method, Na$_2$**L**^{4}·THF$_{0.79}$ (800 mg, 1.39 mmol) and [ZrCl$_4$(THF)$_2$] (564 mg, 1.50 mmol) were used.

Yield = 720 mg, 81%.

Anal. found (Calculated for $C_{32}H_{30}Cl_2N_2O_2Zr$)% C 59.94 (60.36), H 4.75 (4.75), N 4.24 (4.40).

^{1}H NMR 300 MHz (CD_2Cl_2) δ ppm 8.47 (s, 2H, N=C*H*), 7.34 (d, 2H, Ar*H*, $^3J_{HH}$ = 8 Hz), 7.27 (t, 2H, Ar*H*, $^3J_{HH}$ = 8 Hz), 7.20 (dd, 2H, Ar*H*, $^3J_{HH}$ = 8 Hz, $^4J_{HH}$ = 1 Hz), 7.06 (dd, 2H, Ar*H*, $^3J_{HH}$ = 8 Hz, $^4J_{HH}$ = 1 Hz), 6.71 (d, 2H, Ar*H*, $^3J_{HH}$ = 8 Hz), 2.38 (s, 6H, *Me*), 2.26 (s, 6H, *Me*), 2.09 (s, 6H, *Me*).

^{13}C{^{1}H} NMR 75 MHz (CD_2Cl_2) δ ppm 166.9 (N=*C*H), 160.3, 149.6, 139.4, 137.6, 137.5, 131.0, 129.1, 128.6, 125.5, 122.1, 122.0, 121.0 (*Ar*), 19.8 (*Me*), 19.3 (*Me*), 15.7 (*Me*).

IR (Nujol) ν cm^{-1} 2350, 2290, 1587 (m, N=C), 1556, 1401, 1320, 1292 (m, C–O), 1248, 1217, 1159, 1098, 1062, 994, 977, 939, 816, 762, 748, 720, 681, 651, 598, 561.

MS (EI) *m*/*z* 635 [M]$^+$, 600 [M − Cl]$^+$, 585 [M − (Cl and CH$_3$)$^+$].

4.6.5. [Zr**L**^{5}Cl$_2$]

Following the general method, Na$_2$**L**^{5}·HF$_{0.62}$ (800 mg, 1.29 mmol) and [ZrCl$_4$(THF)$_2$] (524 mg, 1.39 mmol) were used.

Yield = 662 mg, 74%.

Anal. found (Calculated for $C_{36}H_{38}Cl_2N_2O_2Zr$)% C 61.75 (62.41), H 5.48 (5.53), N 4.03 (4.04).

^{1}H NMR 300 MHz (CD_2Cl_2) δ ppm 8.57 (s, 2H, N=C*H*), 7.42 (d, 2H, Ar*H*, $^3J_{HH}$ = 8 Hz), 7.27 (t, 2H, Ar*H*, $^3J_{HH}$ = 8 Hz), 7.19 (d, 2H, Ar*H*, $^3J_{HH}$ = 7 Hz), 7.05 (Ar*H*, $^3J_{HH}$ = 8 Hz), 6.83 (d, 2H, Ar*H*, $^3J_{HH}$ = 8 Hz), 3.18 (m, 2H, C*H*Me$_2$, $^3J_{HH}$ = 7 Hz), 2.25 (s, 6H, *Me*), 2.07 (s, 6H, *Me*), 1.29 (d, 6H, CH*Me*$_2$, $^3J_{HH}$ = 7 Hz), 1.14 (d, 6H, CH*Me*$_2$, $^3J_{HH}$ = 7 Hz).

^{13}C{^{1}H} NMR 75 MHz (CD_2Cl_2) δ ppm 166.4 (N=*C*H), 160.1, 149.8, 149.8, 137.6, 137.5, 130.9, 129.0, 128.7, 125.1, 122.0, 119.6, 116.8 (*Ar*), 29.2 (*C*HMe$_2$), 24.4 (CH*Me*$_2$), 23.1 (CH*Me*$_2$), 19.8 (*Me*), 15.8 (*Me*).

IR (Nujol) ν cm^{-1} 2360, 1868, 1583 (s, N=C), 1556, 1404, 1336, 1311, 1258 (s, C–O), 1216, 1156, 1102, 1049, 1019, 996, 939, 897, 875, 836, 817, 793, 778, 761, 754, 739, 727, 686, 657, 625, 571.

MS (EI) *m*/*z* 691 [M]$^+$, 656 [M − Cl]$^+$, 641 [M − (Cl and CH$_3$)]$^+$, 618 [M − (Cl)$_2$]$^+$.

4.6.6. [Zr**L**^{6}Cl$_2$]

Following the general method, Na$_2$**L**^{6}·THF$_{0.59}$ (780 mg, 1.39 mmol) and [ZrCl$_4$(THF)$_2$] (540 mg, 1.43 mmol) were used.

Yield = 497 mg, 56%.

Anal. found (Calculated for $C_{32}H_{30}Cl_2N_2O_2Zr$)% C 60.11 (60.36), H 4.74 (4.75), N 4.30 (4.40).

^{1}H NMR 300 MHz (CD_2Cl_2) δ ppm 8.43 (s, 2H, N=C*H*), 7.82 (t, 2H, Ar*H*, $^3J_{HH}$ = 8 Hz), 7.21 (d, 2H, Ar*H*, $^3J_{HH}$ = 7 Hz), 7.03 (d, 2H, Ar*H*, $^3J_{HH}$ = 7 Hz), 6.65 (s, 2H, Ar*H*), 6.59 (s, 2H, Ar*H*), 2.38 (s, 6H, *Me*), 2.33 (s, 6H, *Me*), 2.08 (s, 6H, *Me*).

^{13}C{^{1}H} NMR 75 MHz (CD_2Cl_2) δ ppm 166.1 (N=*C*H), 161.9, 149.6, 149.2, 141.9, 137.7, 131.0, 129.1, 128.7, 124.3, 122.2, 119.5, 116.9 (*Ar*), 22.0 (*Me*), 19.8 (*Me*), 19.5 (*Me*).

IR (Nujol) ν cm^{-1} 1930, 1606 (N=C), 1585, 1530, 1411, 1391, 1346, 1303, 1256 (w, C–O), 1228, 1209, 1159, 1102, 1072, 1017, 980, 942, 885, 865, 850, 840, 784, 759, 736, 656, 601.

MS (EI) *m*/*z* 636 [M]$^+$, 599 [M − Cl]$^+$.

4.6.7. [Zr**L**^{7}Cl$_2$]

Following the general method, Na$_2$**L**^{7}·THF$_{1.12}$ (800 mg, 1.22 mmol) and [ZrCl$_4$(THF)$_2$] (476 mg, 1.26 mmol) were used.

Yield = 602 mg, 71%.

Anal. found (Calculated for $C_{36}H_{38}Cl_2N_2O_2Zr$)% C 61.48 (62.41), H 5.32 (5.53), N 4.47 (4.04).

^{1}H NMR 300 MHz (CD_2Cl_2) δ ppm 8.43 (s, 2H, N=C*H*), 7.37 (d, 2H, Ar*H*, $^3J_{HH}$ = 8 Hz), 7.25 (t, 2H, Ar*H*, $^3J_{HH}$ = 8 Hz), 7.18 (dd, 2H, Ar*H*, $^3J_{HH}$ = 7 Hz, $^4J_{HH}$ = 1 Hz), 7.08 (dd, 2H, Ar*H*, $^3J_{HH}$ = 7 Hz, $^4J_{HH}$ = 1 Hz), 6.74 (d, 2H, Ar*H*, $^3J_{HH}$ = 8 Hz), 3.33 (m, 2H, C*H*Me$_2$, $^3J_{HH}$ = 7 Hz), 2.37 (s, 6H, *Me*), 2.09 (s, 6H, *Me*), 1.31 (d, 6H, CH*Me*$_2$, $^3J_{HH}$ = 7 Hz), 1.26 (d, 6H, CH*Me*$_2$, $^3J_{HH}$ = 7 Hz).

^{13}C{^{1}H} NMR 75 MHz (CD_2Cl_2) δ ppm 167.2 (N=*C*H), 159.8, 149.5, 139.3, 137.7, 135.9, 133.7, 131.2, 129.0, 128.5, 122.2, 121.8, 121.2 (*Ar*), 28.0 (*C*HMe$_2$), 22.2 (CH*Me*$_2$), 21.8 (CH*Me*$_2$), 19.8 (*Me*), 19.3 (*Me*).

IR (Nujol) ν cm^{-1} 3051, 1953, 1872, 1804, 1600 (m, N=C), 1582, 1557, 1462, 1412, 1393, 1361, 1350, 1310, 1286 (m, C–O), 1258, 1240, 1213, 1162, 1144, 1098, 1058, 1015, 979, 938, 906, 812, 779, 764, 744, 652, 618, 570.

MS (EI) *m*/*z* 692 [M]$^+$, 657 [M − Cl]$^+$, 622 [M − (Cl)$_2$]$^+$.

4.6.8. $[Zr\mathbf{L}^{8}Cl_2]$

Following the general method, $Na_2\mathbf{L}^{8}\cdot THF_{1.23}$ (900 mg, 1.30 mmol) and $[ZrCl_4(THF)_2]$ (500 mg, 1.33 mmol) were used.

Yield = 704 mg, 77%.

Anal. found (Calculated for $C_{38}H_{42}Cl_2N_2O_2Zr$)% C 62.91 (63.31), H 5.95 (5.87), N 3.61 (3.89).

^{1}H NMR 300 MHz (CD_2Cl_2) δ ppm 8.38 (s, 2H, N=C*H*), 7.46 (d, 2H, Ar*H*, $^3J_{HH}$ = 8 Hz), 7.23 (t, 2H, Ar*H*, $^3J_{HH}$ = 8 Hz), 7.17 (d, 2H, Ar*H*, $^3J_{HH}$ = 7 Hz), 7.11 (d, 2H, Ar*H*, $^3J_{HH}$ = 8 Hz), 6.72 (d, 2H, Ar*H*, $^3J_{HH}$ = 8 Hz), 2.35 (s, 6H, *Me*), 2.11 (s, 6H, *Me*), 1.47 (s, 18H, C*Me*$_3$).

^{13}C{^{1}H} NMR 75 MHz (CD_2Cl_2) δ ppm 167.7 (N=*C*H), 161.0, 149.4, 140.0, 137.7, 137.3, 134.3, 131.3, 129.0, 128.5, 122.1, 122.0, 121.7 (*Ar*), 34.8 (*C*Me$_3$), 29.4 (C*Me*$_3$), 19.9 (*Me*), 19.3 (*Me*).

IR (Nujol) ν cm^{-1} 1877, 1598 (N=C), 1580, 1552, 1402, 1384, 1300, 1268 (m, C–O), 1227, 1197, 1138, 1097, 1060, 1030, 978, 937, 904, 833, 816, 803, 780, 763, 743, 648, 618, 564.

MS (EI) *m*/*z* 720 $[M]^+$, 685 $[M - Cl]^+$, 651 $[M - (Cl)_2]^+$.

4.6.9. $[Zr\mathbf{L}^{9}Cl_2]$

Following the general method, $Na_2\mathbf{L}^{9}\cdot THF_{2.35}$ (1.13 g, 1.46 mmol) and $[ZrCl_4(THF)_2]$ (564 mg, 1.50 mmol) were used. After sublimation at 350 °C, 10^{-6} mm Hg, a yellow solid was obtained. Analytical data were obtained on this material. The product was also crystallised from dichloromethane/pentane in similar yield. Single crystals were grown from dichloromethane.

Yield = 420 mg, 40% (From sublimation).

Anal. found (Calculated for $C_{38}H_{42}Cl_2N_2O_2Zr$)% 62.88 (63.31), H 5.83 (5.87), N 3.39 (3.89).

^{1}H NMR 300 MHz (CD_2Cl_2) δ ppm 8.10 (s, 2H, N=C*H*), 7.40 (d, 2H Ar*H*, $^4J_{HH}$ = 2 Hz), 7.22 (t, 2H, Ar*H*, $^3J_{HH}$ = 8 Hz), 7.15 (d, 2H, Ar*H*, $^3J_{HH}$ = 7 Hz), 7.02 (d, 2H, Ar*H*, $^4J_{HH}$ = 2 Hz), 7.01 (d, 2H, Ar*H*), 2.30 (s, 6H, *Me*), 2.06 (s, 6H, *Me*), 1.45 (s, 18H, C*Me*$_3$).

^{13}C{^{1}H} NMR 75 MHz (CD_2Cl_2) δ ppm 170.3 (N=*C*H), 158.7, 149.1, 139.0, 137.9, 136.1, 132.5, 131.1, 129.2, 129.1, 128.6, 123.1, 121.6 (*Ar*), 34.9 (*C*Me$_3$), 29.3 (C*Me*$_3$), 20.5 (*Me*), 19.8 (*Me*).

IR (Nujol) ν cm^{-1} 1610 (N=C), 1590, 1548, 1431, 1410, 1340, 1295, 1269 (m, C–O), 1245, 1210, 1174, 1097, 1036, 1010, 979, 930, 902, 842, 794, 777, 764, 740, 549.

MS (EI) *m*/*z* 720 $[M]^+$, 685 $[M - Cl]^+$, 651 $[M - (Cl)_2]^+$.

4.6.10. $[Zr\mathbf{L}^{10}_2Cl_2]$

Following the general method, $Na\mathbf{L}^{10}\cdot THF_{0.54}$ (567 mg, 1.73 mmol) and $[ZrCl_4(THF)_2]$ (326 mg, 0.86 mmol) were used.

Yield = 461 mg, 77%.

Anal. found (Calculated for $C_{36}H_{40}Cl_2N_2O_2Zr$)% C 61.85 (62.23), H 5.78 (5.80), N 3.78 (4.03).

cis-α-$[Zr\mathbf{L}^{10}_2Cl_2]$ ^{1}H NMR 300 MHz (CD_2Cl_2) δ ppm 8.49 (bs, 2H, N=C*H*), 7.33 (d, 2H, Ar*H*, $^3J_{HH}$ = 8 Hz), 7.10 (br, Ar*H*), 6.65 (d, 2H, Ar*H*, $^3J_{HH}$ = 8 Hz), 2.36 (s, 6H, *Me*), 1.37 (s, 18H, C*Me*$_3$).

cis-α-$[Zr(\mathbf{L}^{10})_2Cl_2]$ ^{13}C{^{1}H} NMR 75 MHz (CD_2Cl_2) δ ppm 167.2 (N=*C*H), 160.2, 151.1, 140.2, 137.4, 134.3, 128.8, 126.9, 123.4, 122.2, 121.9 (*Ar*), 34.7 (*C*Me$_3$), 29.4 (C*Me*$_3$), 19.0 (*Me*).

IR (Nujol) ν cm^{-1} 1601 (m, N=C), 1576, 1555, 1486, 1409, 1362, 1289, 1262 (s, C–O), 1189, 1138, 1059, 1027, 985, 968, 912, 857, 823, 768, 750, 703, 671, 646.

MS (EI) *m*/*z* 694 $[M]^+$, 657 $[M - Cl]^+$, 428 $[M - (\mathbf{L}^{10})]^+$.

4.6.11. $[Zr\mathbf{L}^{11}Cl_2]$

Following the general method, $Na\mathbf{L}^{11}\cdot THF_{0.45}$ (556 mg, 1.73 mmol) and $[ZrCl_4(THF)_2]$ (326 mg, 0.86 mmol) were used. After sublimation at 300 °C, 10^{-6} mm Hg, a yellow solid was obtained.

Yield = 520 mg, 87%.

Anal. found (Calculated for $C_{36}H_{40}Cl_2N_2O_2Zr$)% C 62.10 (62.23), H 5.81 (5.80), N 4.09 (4.03).

cis-α-$[Zr\mathbf{L}^{11}_2Cl_2]$ ^{1}H NMR 300 MHz (CD_2Cl_2) δ ppm 8.13 (bs, 2H, N=C*H*), 7.46 (br, 2H, Ar*H*), 7.29 (br, 4H, Ar*H*), 7.08 (br, 4H, Ar*H*), 6.95 (br, 2H, Ar*H*), 6.84 (br, 2H, Ar*H*), 2.29 (s, 6H, *Me*), 1.34 (s, 18H, C*Me*$_3$).

cis-α-$[Zr\mathbf{L}^{11}_2Cl_2]$ ^{13}C{^{1}H} NMR 75 MHz (CD_2Cl_2) δ ppm 170.6 (N=*C*H), 157.6, 151.0, 139.1, 136.0, 133.1, 129.1, 128.9, 126.9, 123.8, 123.2 (*Ar*), 34.8 (*C*Me$_3$), 29.4 (C*Me*$_3$), 20.5 (*Me*).

IR (Nujol) ν cm^{-1} 1610 (m, N=C), 1588, 1555, 1488, 1435, 1405, 1360, 1334, 1292, 1269 (s, C–O), 1243, 1211, 1192, 1168, 1072, 1027, 984, 964, 906, 862, 844, 795, 776, 763, 702, 688, 618, 554.

MS (EI) *m*/*z* 694 $[M]^+$, 657 $[M - Cl]^+$, 428 $[M - (\mathbf{L}^{11})]^+$.

4.7. Crystallography

Crystals were coated with inert oil and transferred to the cold (180 K) N_2 gas stream on the diffractometer (Bruker-AXS SMART three-circle with CCD area detector). Graphite monochromated Mo K_α radiation λ = 0.71073 Å was used. Absorption correction was performed by multi-scan (SADAB). The structures were solved by direct methods using SHELXS [26] with additional light atoms found by Fourier methods. Crystals of $[Zr\mathbf{L}^{9}Cl_2]$ contained a molecule of dichloromethane disordered over an inversion centre Hydrogen atoms were added at calculated positions and refined using a riding model with freely rotating methyl groups. Anisotropic displacement parameters were used for all non-H atoms; H atoms were given isotropic displacement

parameters $U_{iso}(H) = 1.2U_{eq}(C)$ or $1.5U_{eq}(C)$ for methyl groups. The structures were refined using SHELXL 96 and SHELXTL [27].

Crystallographic data for the structural analysis has been deposited with the Cambridge Crystallographic Data Centre, CCDC 262887–262889.

Acknowledgement

PS thanks EPSRC for support (PDK) and BP for a CASE award (PDK).

References

[1] (a) For example, see: P.R. Woodman, N.W. Alcock, I.J. Munslow, C.J. Sanders, P. Scott, J. Chem. Soc., Dalton Trans. (2000) 3340;
(b) P.A. Cameron, V.C. Gibson, C. Redshaw, J.A. Segal, A.J.P. White, D.J. Williams, J. Chem. Soc., Dalton Trans. (2002) 415;
(c) D.G. Black, D.C. Swenson, R.F. Jordan, Organometallics 14 (1995) 3539;
(d) H. Tsurugi, Y. Matsuo, T. Yamagata, K. Mashima, Organometallics 23 (2004) 2797.

[2] (a) P.D. Knight, C. Morton, K.M. Gillespie, P. Scott, Chem. Commun. (2003) 1770;
(b) P.N. O'Shaughnessy, P. Scott, Tetrahedron: Asymmetry 14 (2003) 1979;
(c) P.D. Knight, I.J. Munslow, P.N. O'Shaughnessy, P. Scott, Chem. Commun. (2004) 894;
(d) P.N. O'Shaughnessy, K.M. Gillespie, P.D. Knight, C. Morton, P. Scott, J. Chem. Soc., Dalton Trans. (2004) 2251.

[3] (a) S. Matsui, T. Fujita, Catal. Today 66 (2001) 63;
(b) G.W. Coates, J. Chem. Soc., Dalton Trans. (2002) 467;
(c) H. Makio, N. Kashiwa, T. Fujita, Adv. Synth. Catal. 344 (2002) 477;
(d) Y. Suzuki, H. Terao, T. Fujita, Bull. Chem. Soc. Jpn. 76 (2003) 1493;
(e) M. Mitani, J. Saito, S.I. Ishii, Y. Nakayama, H. Makio, N. Matsukawa, S. Matsui, J.I. Mohri, R. Furuyama, H. Terao, H. Bando, H. Tanaka, T. Fujita, Chem. Rec. 4 (2004) 137.

[4] H. Makio, T. Fujita, Macromol. Symp. 213 (2004) 221.

[5] S. Reinartz, A.F. Mason, E.B. Lobkovsky, G.W. Coates, Organometallics 22 (2003) 2542.

[6] P.D. Knight, A.J. Clarke, B.S. Kimberley, R.A. Jackson, P. Scott, Chem. Commun. (2002) 352.

[7] P.D. Knight, P.N. O'Shaughnessy, I.J. Munslow, B.S. Kimberley, P. Scott, J. Organomet. Chem. 683 (2003) 103.

[8] L. Blank, Statistical Procedures for Engineering, Management and Science, McGraw-Hill, New York, first ed., pp. 487–515 (Chapter 27);
L.C. Hamilton, Regression With Graphics – A Second Course in Applied Statistics, Brooks/Cole, Belmont, CA, first ed., pp. 29–64 (Chapter 2).

[9] F.O. Rice, K.F. Herzfeld, J. Am. Chem. Soc. 56 (1934) 284.

[10] K.J. Laidler, Chemical Kinetics, third ed., Harper & Row, New York, 1995, Section 8.5.

[11] P.R. Woodman, C.J. Sanders, N.W. Alcock, P.B. Hitchcock, P. Scott, New J. Chem. 23 (1999) 815.

[12] P.R. Woodman, I.J. Munslow, P.B. Hitchcock, P. Scott, J. Chem. Soc., Dalton Trans. (1999) 4069.

[13] T.R. Younkin, E.F. Conner, J.I. Henderson, S.K. Friedrich, R.H. Grubbs, D.A. Bansleben, Science 287 (2000) 460.

[14] G.J.P. Britovsek, V.C. Gibson, D.F. Wass, Angew. Chem., Int. Ed. 38 (1999) 428.

[15] P.-J. Sinnema, T.P. Spaniol, J. Okuda, J. Organomet. Chem. 598 (2000) 179.

[16] S. Matsui, M. Mitani, J. Saito, Y. Tohi, H. Makio, N. Matsukawa, Y. Takagi, K. Tsuru, M. Nitabaru, T. Nakano, H. Tanaka, N. Kashiwa, T. Fujita, J. Am. Chem. Soc. 123 (2001) 6847.

[17] (a) C.A. Hunter, J.K.M. Sanders, J. Am. Chem. Soc. 112 (1990) 5525;
(b) C. Janiak, J. Chem. Soc., Dalton Trans. (2000) 3885;
(c) H. Suezawa, T. Yoshida, Y. Umezawa, S. Tsuboyama, M. Nishio, Eur. J. Inorg. Chem. (2002) 3148.

[18] (a) D.G. Bickley, N. Serpone, Inorg. Chem. 18 (1979) 2200;
(b) I.J. Munslow, A.J. Clarke, R.J. Deeth, I. Westmoreland, P. Scott, Chem. Commun. (2002) 1868.

[19] D.A. Pennington, W. Clegg, S.J. Coles, R.W. Hartington, M.B. Hursthouse, D.L. Hughes, M.E. Light, M. Schormann, M. Bochmann, S.J. Lancaster, J. Chem. Soc., Dalton Trans. (2005) 561.

[20] N. Matsukawa, S. Matsui, M. Mitani, J. Saito, K. Tsuru, N. Kashiwa, T. Fujita, J. Mol. Catal. A 169 (2001) 99.

[21] D.W. Carpenetti, L. Kloppenburg, J.T. Kupec, J.L. Petersen, Organometallics 15 (1996) 1572.

[22] (a) R.R. Schrock, J.D. Fellmann, J. Am. Chem. Soc. 100 (1978) 3359;
(b) Available from: <http://www.syntheticpages.org/pages/120>.

[23] (a) P.J. Davidson, M.F. Lappert, R. Pearce, J. Organomet. Chem. 57 (1973) 269;
(b) Available from: <http://www.syntheticpages.org/pages/135>.

[24] (a) U. Zucchini, E. Albizzati, U. Giannini, J. Organomet. Chem. 26 (1971) 357;
(b) Available from: <http://www.syntheticpages.org/pages/1>.

[25] N.U. Hofsløkken, L. Skattebøl, Acta Chem. Scand. 53 (1999) 258.

[26] G.M. Sheldrick, SHELXTL Ver 5.1, Bruker Analytical X-ray Systems, 1997.

[27] G.M. Sheldrick, Acta Crystallogr., Sect. A 46 (1990) 467.